High-performance multifunctional electrospun fibrous air filter for personal protection: A review

Zungui Shao [a], Huatan Chen [a], Qingfeng Wang [a], Guoyi Kang [a], Xiang Wang [b], Wenwang Li [b], Yifang Liu [a], Gaofeng Zheng [a],*

[a] Department of Instrumental and Electrical Engineering, Xiamen University, Xiamen 361102, China
[b] School of Mechanical and Automotive Engineering, Xiamen University of Technology, Xiamen 361024, China

ARTICLE INFO

ABSTRACT

With the increasingly serious air pollution and the rampant coronavirus disease 2019 (COVID–19), preparing high–performance air filter to achieve the effective personal protection has become a research hotspot. Electrospun nanofibrous membrane has become the first choice of air filter because of its small diameter, high specific surface area and porosity. However, improving the filtration performance of the filter only cannot meet the personal needs: it should be given more functions based on high filtration performance to maximize the personal benefits, called, multifunctional, which can also be easily realized by electrospinning technology, and has attracted much attention. In this review, the filtration mechanism of high–performance electrospun air filter is innovatively summarized from the perspective of membrane. On this basis, the specific preparation process, advantages and disadvantages are analyzed in detail. Furthermore, other functions required for achieving maximum personal protection benefits are introduced specifically, and the existing high–performance electrospun air filter with multiple functions are summarized. Finally, the challenges, limitations, and development trends of manufacturing high–performance air filter with multiple functions for personal protection are presented.

1. Introduction

In recent years, the global environment is deteriorating, and air pollution is becoming more and more serious due to the development of industrialization. Even worse, the coronavirus disease 2019 (COVID–19) continues to erupt and mutate, seriously threatening public health [1–3]. Air filter (i.e., membrane used for air filtration) is the key to personal protection [4]. By filtering small particles in the air, respiratory diseases can be avoided directly and effectively [5]. Therefore, the development of high–performance air filter has always been a research hotspot [6–8].

As an important equipment for personal protection, masks are widely worn in daily life to prevent particles in the air, where the core filter layer plays a major role in filtering [9,10]. Fibrous membranes have most widely used in air filtration because of its small pore size, high porosity and universality of materials, which are expected to be used as the core filter layer of masks [11,12]. High filtration efficiency is an important capability of air filter [13]. However, most preparation methods of fibrous filter cannot realize the filtration of ultrafine particles in low resistance due to the relatively large pores and fiber diameters (e.g. synthesis, spin–bonding and melt blowing) [14]. Therefore, the core filter layer of traditional commercial mask (i.e., polypropylene (PP) melt–blown microfibrous membrane) is endowed with electrostatic adsorption capacity by a high–voltage corona discharge electret technology, so as to achieve a satisfactory filtration performance [15]. Unfortunately, the materials available for the melt–blown electret method are very limited, and the electrostatic charge is easily dissipated due to moisture, resulting in a sharp decline in filtration efficiency [16,17]. Hence, nanofibrous membrane with more stable filtration performance have become a better choice for personal protection [18]. Electrospinning is a general and low–cost method for easily preparing nanofibrous membrane with large specific surface area, small pore size, controllable fiber diameter (particularly, it can realize the stable preparation of nanofibers below 100 nm), and relatively high production rate [19]. Moreover, there are many kinds of materials available for electrospinning, including various polymers, small

molecules, ceramics and so on, which makes it possible to quickly pre-pare nanofibers with various structures and functions [20–24]. Thus, more and more electrospun nanofibrous membrane are manufactured to realize high–performance air filtration and used for personal protection [25–27].

In the last decade, electrospun nanofibrous membranes with high filtration efficiency and low resistance have been widely studied because they can match the protection and comfort of users simultaneously [28]. Generally, it can be realized through structural regulation and fibrous modification [29]. Nowadays, with the continuous development of related research, high filtration efficiency and low resistance air filtra-tion has been deeply rooted in the hearts of the people: the first thing we think of the high–performance electrospun nanofibrous membrane is its high filtration efficiency and low resistance, that is, the existing high-–performance air filter has been defaulted to possess high filtration ef-ficiency and low resistance [30–32]. Nevertheless, extremely good filtration performance is no longer the goal pursued by researchers: evaluating the performance of air filter should be comprehensive [10]. For personal protection, the assessment of air filter should consider the comprehensiveness of protection and higher comfort [6]. Therefore, on the basis of high filtration efficiency and low resistance, the high-–performance air filter for personal protection should be given more functions [14]. In other words, high–performance filters for personal protection are multifunctional. For example, the air filter with anti-bacterial properties can prevent the harm of bacteria to the human body; the adsorption capacity of volatile organic compounds (VOCs) will protect the human body from being poisoned by inhaling harmful gases (e.g., formaldehyde and sulfur dioxide (SO_2)) [33–36]. Ultimately, air filter integrating all functions that beneficial to personal protection is needed, which will also maximize the benefits for personal protection [37,38]. Multifunction coupling with high filtration performance is a complex process, which requires deeply explored each mechanism. In recent years, there have been many reviews on high–performance electrospun air filter. For example, Ding's group discussed the rela-tionship of structure and electrostatic effect to filtration performance [39]; Zhao's group summarized several different types of electro-spinning technology, the structure and characteristics of high-–performance air filtration membranes, and some application scenarios [5]; Huang's group introduced high–performance air filter with different structures and prepared by various bio–based materials, and listed many functions and applications [13,14,30]. However, at present, there is no in–depth summary of high–performance electrospun air filter used for personal protection, and the mechanism of air filtration was not well summarized: all explanations were based on the analysis of single fiber model, which could not reasonably explain the necessary condi-tions for high efficiency and low resistance air filtration. Thus, in–depth explanation of the mechanism of high–efficiency and low–resistance air filtration, and analysis of strategies that can maximize the benefits of personal protection (i.e., taking both protection and comfort into ac-count) will help people better use masks to resist threats from various air pollutants.

In this review, we summarized the high air filtration performance mechanisms from the perspective of membrane, and other required functions of electrospun nanofibrous air filter for maximizing the ben-efits of personal protection. Firstly, the electrospinning process and mechanisms of high–performance air filtration were introduced in detail, and the existing strategies were deeply analyzed; then, other functions of electrospun air filter required for personal protection were listed; finally, the current problems and future developments of high-–performance multifunctional electrospun air filter for personal pro-tection were discussed.

2. Mechanisms of high filtration performance electrospun air filter

For air filter, filtration capacity is the most important performance

[40]. However, in exchange for high filtration efficiency with thick and tight fibrous accumulation, it will make breathing difficult or even suffocate [41]. Therefore, filtration with high efficiency and low resis-tance has become the basic demand of high–performance electrospun air filter for personal protection [42–44]. Next, the preparation process and filtration performance of electrospun air filter will be introduced in detail.

2.1. Electrospinning process

Electrospinning is a simple method to prepare nanofibrous mem-branes, which mainly includes high–voltage power supply, syringe pump, spinneret and collector [45]. Under high–voltage electrical field, the polymer solution charged and deformed into suspended droplet [46]. When the voltage applied at the end of the spinneret exceeds a certain critical value, the droplet changes into a Taylor cone and jets appeared [47]. Then the jets are stretched in violent whipping and so-lidified into nanofibers at high speed [48].

The morphologies and properties of electrospun nanofibers and their aggregates (i.e., nanofibrous membranes) can be easily controlled by adjusting the properties of electrospinning solution (e.g., solute types, polymer relative molecular mass, solvent, concentration, viscosity, surface tension, and conductivity), process parameters (e.g., voltage, supplied rate, and collecting distance), and environmental parameters (e.g., temperature and humidity) [49]. Based on this, nanofibrous membranes with various properties and functions are easily prepared through electrospinning [50–52].

2.2. Filtration mechanism

The classical filtration theory simulates the air filter as an aggregate composed of several single cylinders to study the filtration process [30]. Specifically, it is mainly divided into interception, inertial impaction, Brownian diffusion, gravity deposition, and electrostatic absorption, as shown in Fig. 1 [53]. Among them, electrostatic adsorption and Brow-nian diffusion play a major role in ultrafine particle (<0.3 μm) filtration [54]; interception and inertial impaction have great influence on par-ticles larger than 0.3 μm [14]; gravity deposition is usually negligible due to its weak force for small size particles [53]. Furthermore, screening is supplemented as another major filtration function of fibrous aggregate (i.e. fibrous membrane), which intercepts particles by the pore formed by overlapping between fibers, or the filter cake formed by deposited particles; it mainly intercepts particles smaller than the pore size of the filter layer through physical interception [55].

The filtration process of fibrous filter is synergized by the above ef-fects. The filtration efficiency (η) is expressed by Kuwabara model [56], as following:

$$\eta = 1 - \exp\left[\frac{-4\theta\alpha T}{\pi D(1-\alpha)}\right] \tag{1}$$

where, θ is the filtration efficiency of single fiber, α is the fibrous volume fraction, T is the thickness of air filter, and D is the average diameter of fiber. According to the Kuwabara model, increasing the thickness of filter and decreasing the diameter of fibers will improve the filtration efficiency.

2.3. Pressure drop

The pressure drop is used to indicate the resistance of air flowing through the fibrous filter, which is represented by the following formula [57]:

$$\Delta p = 64\mu v \frac{1}{D^2}\alpha^{1.5}(1 + 56\alpha^3)T \tag{2}$$

where, Δp is the resistance (i.e., pressure drop), μ is the air viscosity and
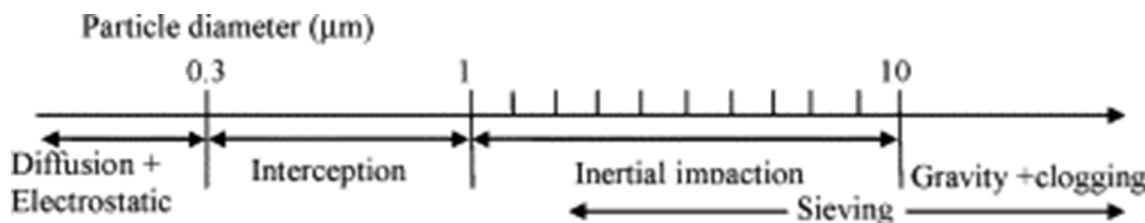
Fig. 1. Operative particle size in various interaction mechanisms [53].

v is the face velocity across the air filter.

Thicker filters and finer fibers are close accumulation, affecting the passage of air flow, resulting in high resistance. Therefore, it is necessary to adjust the structure and parameters of the fibrous filter, realizing the optimized air flow field and lower resistance.

2.4. Slip effect

Generally, electrospun nanofibrous air filter has lower resistance compared to microfibrous one, which is attributed to the slip effect: the airflow bypasses the nanofibers, reducing the resistance [58]. Four states of air flow near a single fiber are judged by Knudsen number (K_n), as following:

$$K_n = \frac{2\lambda}{d} \tag{3}$$

where, λ is the mean free path of air molecules (about 66 nm), and d is the fibrous diameter.

Specifically, When $d > 132$ μm, $K_n < 0.001$, the air flow is in a continuous flow regime and completely impacts the fiber so that the resistance produced; when 528 nm $< d <$ 132 μm, $0.001 < K_n < 0.25$, the airflow is in the slip flow regime, bypassing occurs, and the resistance is reduced, which is called the slip effect; when 13.2 nm $< d <$ 528 nm, $0.25 < K_n < 10$, the airflow is in an transition regime, the slip effect is enhanced and the resistance is further reduced; when $d <$ 13.2 nm, $K_n > 10$, the air flow is in the free molecular regime, and the slip effect is the strongest [59]. The existence of fiber does not affect the streamline, and there is almost no resistance, as shown in Fig. 2 [60]. Therefore, the

smaller the diameter of single fiber, the stronger the slip effect, and it is expected to realize the air filtration process with low resistance [61,62]. Bao et al. verified the impact of slip effect on reducing pressure drop based on experiments for the first time, which was by distinguishing the influences of inhomogeneity at low–pressure conditions [63]. Nowadays, the contribution of slip effect to reducing the pressure drop of fibrous membrane has been widely accepted [7,14,30].

Nevertheless, the stacking of fibers will affect the slip effect: when the fibers are stacked too densely, the air flow has no place to bypass, which will greatly reduce the slip effect [41]. Therefore, small fiber diameter and sufficient fiber spacing are the key to achieve enhanced slip effect.

Generally, porosity (φ) is used to characterize the fluffy degree of fibrous accumulation, as following [64]:

$$\varphi(\%) = (1 - \frac{\rho_0}{\rho}) \times 100\% \tag{4}$$

where, ρ_0 and ρ are the volume density and density of the material, respectively.

The higher the porosity is, the fluffier the fibrous membrane is. In general, nanofibrous membranes with high porosity often have strong slip effect, because there is enough space between the fibers [65].

2.5. Filtration with high efficiency and low resistance

The comprehensive performance of air filter is evaluated by quality factor (QF), as following [66]:
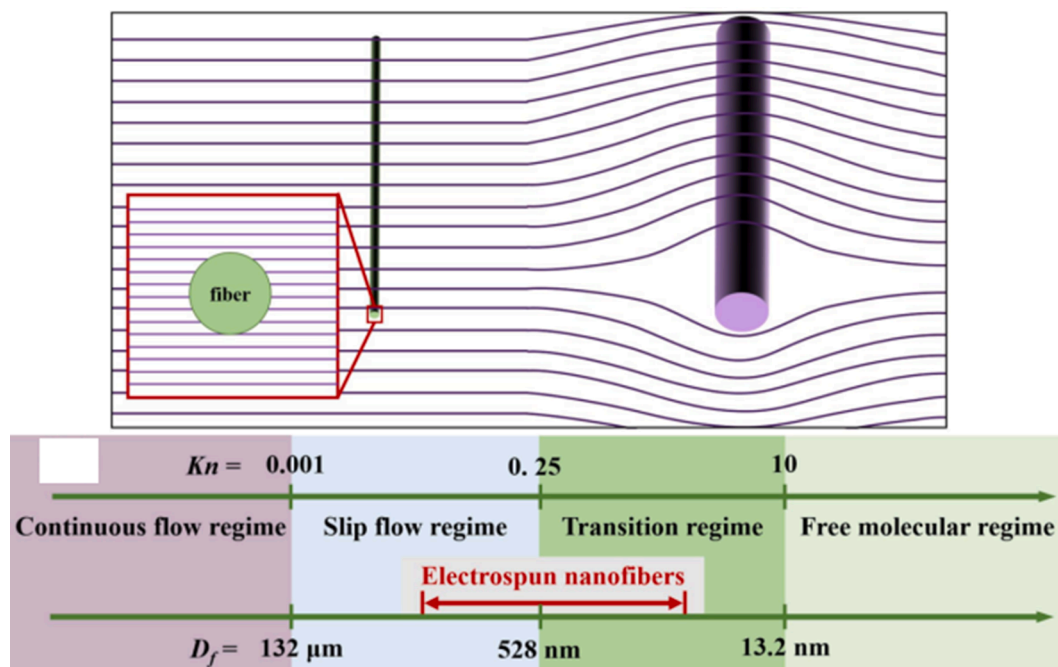
Fig. 2. Theoretical diagram of slip effect of single fiber. Where, K_n and D_f stands for Knudsen Number and the diameter of fibers, respectively [60].

$$QF(Pa^{-1}) = -\frac{\ln(1-\eta)}{\Delta p}, \quad (5)$$

When the filtration efficiency is higher and the air resistance is lower, the QF is higher and the air filtration performance is better.

Currently, in the same case, electrospun air filter which QF is better than commercial high efficiency particulate air filter (HEPA) can be regarded owing high filtration performance [13]. Particularly, existing studies have widely used specific conditions (i.e., for 0.3 μm NaCl particles under air flow of 32 L/min or velocity of 5.3 cm/s) to characterize the filtration performance of electrospun air filter, under which their QFs are generally higher than the commercial meltblown masks [41,67–69].

For high filtration performance electrospun air filter, enhanced filtration effects and low resistance are essential [70]. However, the existing filtration theory based on single fiber cannot well explain the high filtration performance reasons of electrospun nanofibrous membrane. Therefore, we combine the filtration mechanism and air flow field analysis to consider the filtration process of nanofibrous membrane, then summarized the mechanisms based on existing literature.

Generally, the filtration of larger particles (>0.3 μm) can be easily achieved through the interception and screening of the pore of nanofibrous membrane, but this is not very helpful to improve the overall filtration efficiency [71]. On the contrary, improving the filtration efficiency of the most penetrating particles (<0.3 μm) will effectively promote the overall filtration capacity of the air filter, which can be achieved by strengthening the Brownian diffusion (i.e., the phenomenon that particles break away from the air flow line and move irregularly, the smaller the particle, the stronger the Brownian diffusion) and electrostatic absorption [72,73]. Among them, the electrostatic absorption is not affected by the air flow field, and has a strong attraction for ultrafine particles [57]. In addition, when particles are deposited on the fiber by Brownian diffusion, they may fall off due to the smoothness of the fiber surface. Thus, improving the roughness of fibers (i.e., fibers with rough structure) can increase the contact area between particles and fibers, thus making particles more firmly intercepted on the surface of fiber, which is another effective method to improve the filtration capacity [74–77]. In this case, the air flow field is less negatively affected compared to smooth fibers, thus the filtration performance improved. These called improving the initiative of the fibers.

On the other hand, the particle filtration process also needs to consider the influence of air flow field, because the slip effect widely exists in electrospun nanofibrous membrane, its influence on particle behavior cannot be ignored [58]. It has become a widespread consensus that the slip effect makes the nanofibrous membrane more breathable [59–61]. However, the airflow bypass may also make the particles bypass the fiber, which may have an adverse impact on the filtration. Jung et al. proved that the enhanced slip effect will make the air flow field closer to the surface of fiber, thus the filtration efficiency caused by Brownian diffusion is increased [78]. Therefore, the filtration efficiency of ultrafine particles will not be weakened by the slip effect, because they are not easy to follow the air streamline [54]. On the contrary, Brownian diffusion enhanced by slip effect will also promote the filtration of ultrafine particles. For larger particles, it is also easy to be intercepted by the tortuous pores of the nanofibrous membrane in the subsequent filtration process. In general, slip effect has a positive contribution to the improvement of overall filtration efficiency, and its contribution to high efficiency and low resistance air filtration has also been supported by the literature [61]. It is worth noting that most of the existing studies (as described in Section 3.2) attribute the reduction of air resistance to the enhancement of slip effect, but do not involve its contribution to the improvement of air filtration efficiency too much: the research in this part is relatively scarce.

To sum up, high efficiency and low resistance air filtration process
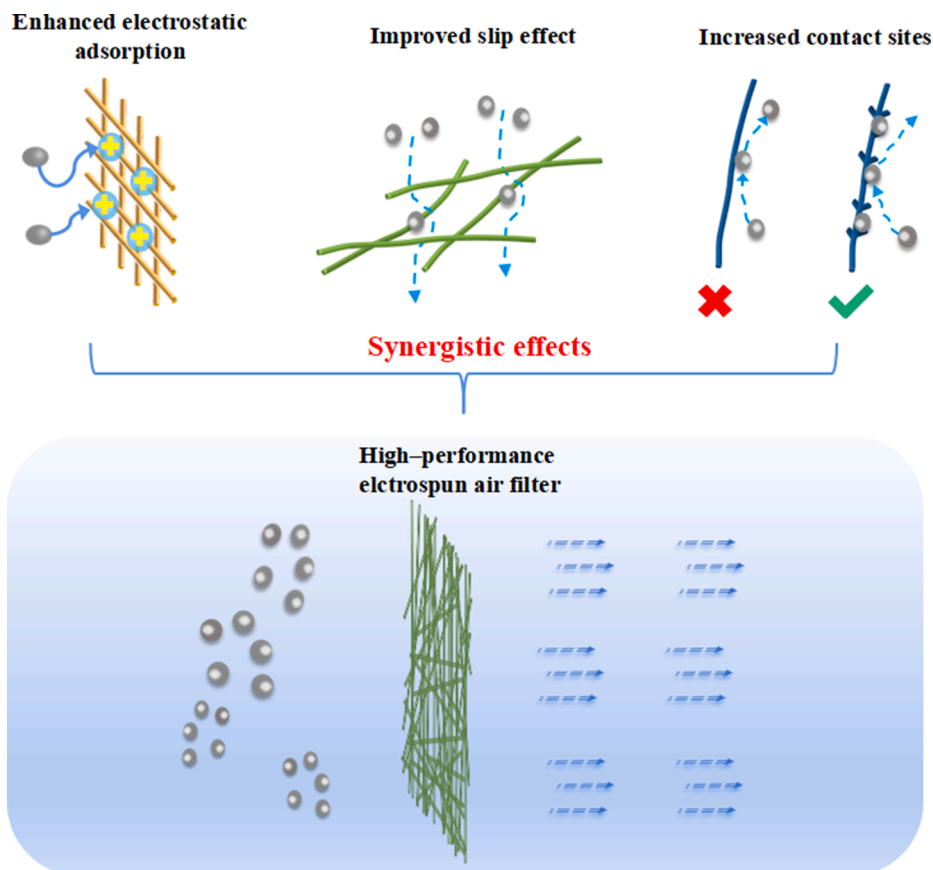
Fig. 3. Three synergistic effects of fibrous membrane to enhance air filtration performance.

requires synergistic effects among electrostatic adsorption, slip effect, and contact sites between fibers and particles, as shown in Fig. 3. Though it is still difficult to quantify the contribution of these three mechanisms to air filtration.

3. Preparation of electrospun nanofibrous air filter with high efficiency and low resistance

As mentioned earlier, enhanced electrostatic adsorption and slip effect, and high roughness of fibers are the three mechanisms to realize high–efficiency and low–resistance air filtration. Next, the specific mechanism and the realization method of electrospinning will be introduced in detail.

3.1. Function of enhanced electrostatic adsorption

Generally, electrospun nanofibers will initially have significant electrostatic adsorption capacity due to the influence of high voltage, and these injected charges will gradually decay and disappear within 24 h [14]. In this case, such nanofibers are not considered to have enhanced electrostatic adsorption. The situations discussed below ensure that the nanofibers have stable electrostatic adsorption capacity.

Usually, fibrous filters improve the filtration efficiency by increasing the density and thickness, but this will also increase the resistance sharply [79]. Fortunately, electrostatic enhanced air filters can achieve higher particle capture efficiency without increasing resistance [80]. Thus, the filtration performance of the air filter will be greatly improved.

3.1.1. Electret with space charge

In the electrospinning process, the charge will be spontaneously embedded on the surface traps of the medium in the electric field, which is called space charge [81]. When the medium has high dielectric constant, the space charge can be well retained for a long time to form monopolar electrets [82]. At present, space charge electret is realized by

adding electret particles (e.g., silicon dioxide (SiO_2); titanium dioxide (TiO_2); barium titanate ($BaTiO_3$); silicon nitride (Si_3N_4); attapulgite; boehmite; polytetrafluoroethylene (PTFE); hydroxylapatite (HAP)) [79,83–89], electrospinning nonpolar fibers (e.g., PTFE; polystyrene (PS) and polyvinyl chloride (PVC)) [90–92], and realizing interface polarization between polar and nonpolar mediums [93,94].

By adding electret particles, electrospun air filters can easily achieve enhanced electrostatic adsorption capacity. Li et al. developed electrospun electreted PEI fibrous air filter with high filtration performance by introducing SiO_2 nanoparticle electrets for the first time, as shown in Fig. 4(a). The air filtration performance of as–prepared membrane was much better than that of commercial filter. The filtration efficiency for 300 nm aerosol particles was 99.992 %, the pressure drop was only 61 Pa, and the QF was 0.155 Pa^{-1}. Furthermore, SiO_2 nanoparticles could capture more space charges, showing the highest surface potential and the slowest attenuation, as shown in Fig. 4(b) [83]. The particle electret air filter is easy to realize the strong electrostatic adsorption capacity brought by high filling density [81]. However, the problem of agglomeration and uneven distribution of particles will also make the performance of air filter unstable. Worse, the introduction of electret particles also has the risk of nanotoxicity and desorption, which may endanger human health [93].

The preparation of all–polymer nonpolar electret nanofibers is an effective method to avoid above problems. Chen et al. constructed multilevel structured thermoplastic polyurethanes/polystyrene/polyamide–6 (TPU/PS/PA–6) composite membrane. The synergistic effect of mechanical filtration and strong electrostatic adsorption realized high–efficiency and low–resistance air filtration, in which PS electret layer was the main filtration function layer, providing strong filtration capacity. The filtration efficiency for 0.3 μm NaCl particles was 99.99 %, the air resistance was 54 Pa, and the QF was 0.17 Pa^{-1} [68]. However, it is difficult for nonpolar electret fibers to achieve high filtration efficiency alone, because the deposition of fibers is difficult due to charge repulsion [68].
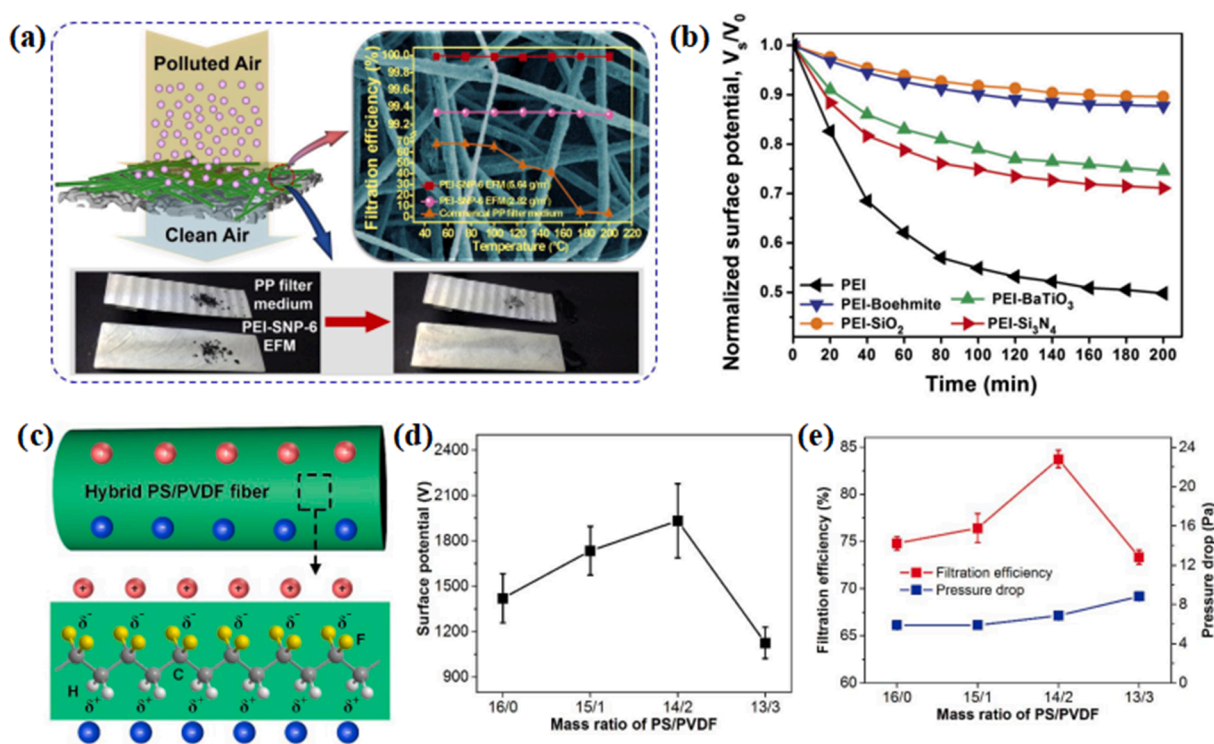
Fig. 4. (a) Schematic diagram of PEI/SiO_2 nanofibrous membrane, and the filtration efficiency of different membranes under different temperatures. (b) Surface potential decay of different hybrid membranes at room temperature over time [83]. (c) Schematic illustrating the contribution of PVDF on electret effect. (d) Surface potentials of PS/PVDF electret fibers with different mass ratio. (e) Filtration efficiency and pressure drop of PS/PVDF membranes with different mass ratio [93].

Fortunately, the all–polymer electret fiber preparation strategy based on the combination of polar and non–polar medium can effectively realize high–efficiency air filtration through interface polarization [93]. That is due to the different electrical properties (i.e., permittivity and conductivity) of the two phases in the medium, resulting in the accumulation of free charges on the two–phase interface under the action of an electric field [86]. Li et al. prepared all–polymer hybrid PS and polyvinylidene fluoride (PVDF) electret fibers by studying the complementarity of electrical response between electrospun polymers. The different electron transport ability between PVDF and PS made the charge accumulate in the interface region rather than transfer from one to another. Therefore, an induced charge in the same direction as the injected charge was generated in the PS, thereby enhancing the electret effect, as shown in Fig. 4(d). The surface potential was increased by 36 % through introducing 2 / 16 content of PVDF, as shown in Fig. 4 (e), thus the filtration efficiency was 12 % higher than that of PS fiber only, as shown in Fig. 4(f). Finally, the filtration efficiency was 99.752 %, the resistance was 72 Pa, and the QF was 0.083 Pa^{-1} [93].

The space charge electret air filter has high filtration performance because of the long–range intermolecular force, but the space charge is also easy to dissipate due to the influence of the environment (e.g., high temperature and humidity), and reduces the filtration performance [95–97]. Moreover, the non–renewable charge is its fatal disadvantage, which hinders the reuse [98].

3.1.2. Induced dipole charge

Polar materials with high dipole moment can spontaneously arrange to form permanent dipoles under the influence of electric field, so as to induce dipole charge, which is more stable than space charge [99]. At present, many materials have been electrospun into induced dipole charge air filters, such as polyacrylonitrile (PAN), polybenzimidazole (PBI), PVDF and so on [100–102]. Lee et al. reported electrospun PBI nanofibrous membrane with high electric dipole moment (6.12 D), as shown in Fig. 5(a). Compared with PA–6 electrospun air filter (3.31 D) and PP commercial filter (0.35 D) with lower dipole moment, the surface potential of PBI electrospun nanofibrous membrane (0.77 V) was more than 1.5 times higher (PA–6 = 0.492 V and PP = –0.374 V), as shown in Fig. 5(b). The filtration efficiency of PBI air filter was 98.5 %, the pressure drop was 130 Pa, and the QF was 0.032 Pa^{-1}, as shown in Fig. 5 (c), exhibiting three times the air filtration performance of commercial masks because of stronger electrostatic adsorption [102].

Similarly, it still faces the problem of non–renewable charge. For this reason, Ding et al. introduced photochromic spiropyran (SP) and constructed SP/PS nanofibrous air filter with spontaneous induced electrostatic charge. Spontaneous polarization of photochromic molecules under different wavelengths of light could induce surface charge in electret material, the dipole moment could be increased from 5.4 D to 19. 54 D, as shown in Fig. 5(d). After washing, the surface potential of SP/PS fabrics irradiated by ultraviolet light also showed higher surface potential (~250 V) than PS and PP fabrics (before washing ~ 230 V, after washing ~ 37.2 V), as shown in Fig. 5(e). Thus, after repeated washing, the filtration efficiency of SP/PS fibrous membrane was always maintained at more than 95 %, the resistance was less than 343.2 Pa, while the filtration efficiency of PS was reduced to less than 90 %, as shown in Fig. 5(f) [99]. Therefore, this strategy further broadens the application of dipole induced electret. However, the limitation of
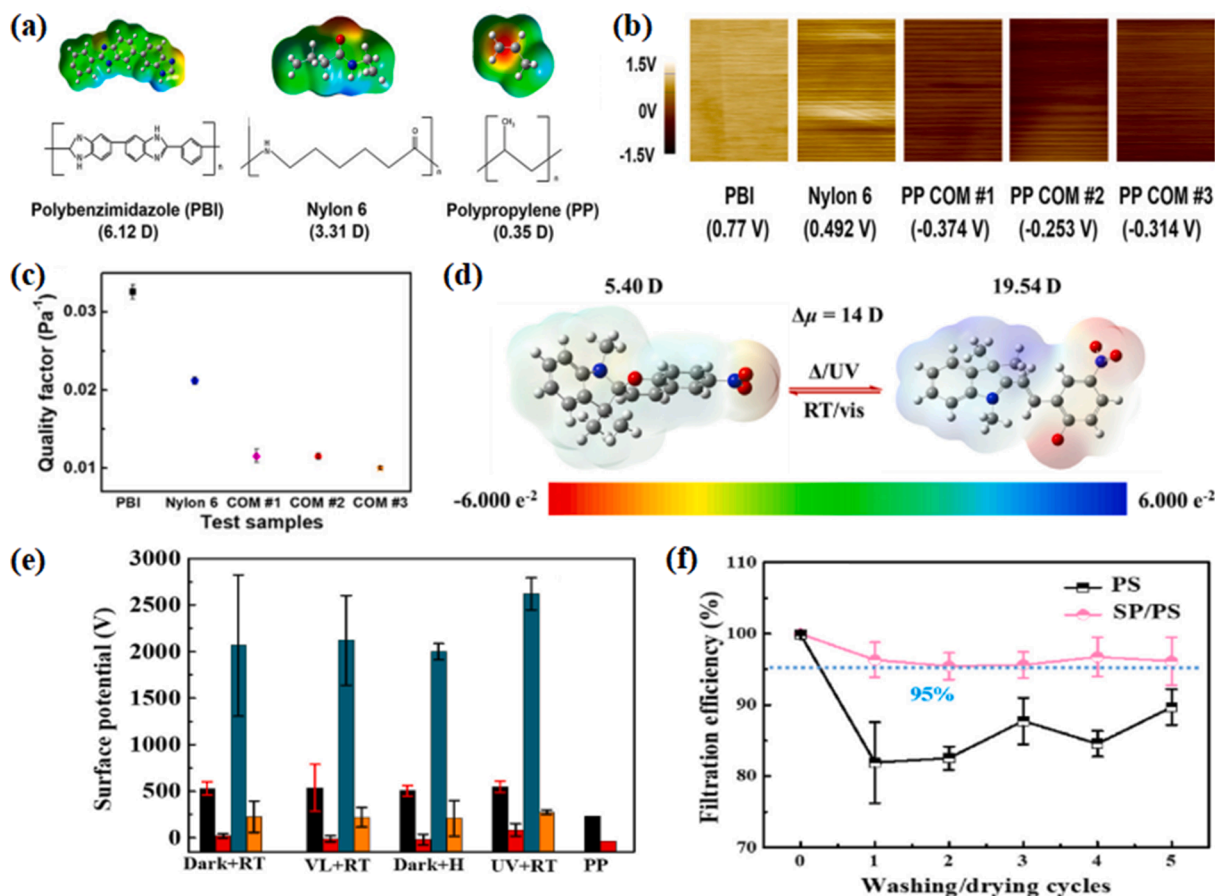
Fig. 5. (a) Molecular structures and dipole moment of PBI (6.12 D), Nylon–6 (3.31 D), and PP (0.35 D). (b) Kelvin probe force microscopy images of surface potential of PBI, Nylon–6 nanofiber filters, and three PP commercial filters. (c) Quality factors (QFs) of different filters [102]. (d) Interconversion between optimized molecular structures of spiropyran (SP, left)/merocyanine (right) induced by different light irradiation. (e) Surface potential changes of SP/PS composite fabrics washed by water under different lighting conditions. (f) Stability of filtration efficiency of fabrics after being washed by 75% ethanol and dried for 5 times [99].

materials has a great obstacle to the promotion of this strategy (e.g., there are fewer choices of materials). Although the dipole charge electret has better electrical stability, its electrostatic adsorption performance still has room to improve compared with the space charge electret due to finite short–range intermolecular force [81].

3.1.3. Friction induced charge

Friction induced charge is formed by friction between materials with different electronegativity, which called triboelectrification [103]. Its biggest advantage is that the charge can be regenerated, avoiding the problem of reduced air filtration performance due to charge dissipation. According to the research of Wang et al., triboelectrification is the result of electron transfer [104]. Theoretically, electron transfer will occur between the two materials with electronegativity differences: the materials with strong electronegativity will be negatively charged and the weak one will be positively charged [105]. At this time, the fiber will carry a net charge to adsorb particles in the air [57]. Liu et al. prepared the self–powered electrostatic adsorption mask (R–TENG) based on triboelectric nanogenerator for the first time, which depended on friction between copper (Cu) and PVDF in contact and separation modes, as shown in Fig. 6(a). For the particulates in sizes of 0.5 μm and below, the removal efficiency of R–TENG decreased only from 98 to 88.9 wt% in

240 min, while that of PVDF membrane decreased rapidly from 97.4 to 62.4 wt%, as shown in Fig. 6(b). At the same time, the surface potential retention ability of R–TENG was better: when the test time increased from 0 to 240 min, the potential decreased from –600 to –190 V and remained stable, while that of PVDF membrane decreased from –600 V to 0, indicating that R–TENG had stronger electrostatic adsorption, as shown in Fig. 6(c) [106]. Subsequently, our group simplified the structure of friction induced charge air filter. Enhanced self–powered electrostatic adsorption air filter was electrospun by compositing PA6 and PVC (PA6/PVC) nanofibrous membrane, where PA6 has weak electronegativity and PVC has strong one, thus, PA6 showed positive charge on the surface and PVC showed negative one, as shown in Fig. 6(d).

With the increasing base weight of the PA6/PVC composite membrane, the friction effect was enhanced, so that the voltage increased. Compared with the uncharged membrane, the self–powered membrane had a larger voltage value, as shown in Fig. 6(e). The QF of the self––powered membrane was 0.0974 Pa^{-1}, which was 8.46 % higher than that of the non–charged one, as shown in Fig. 6(f) [107]. Under the action of air flow or flapping, the self–powered electrostatic adsorption air filter can be easily charged to realize charge regeneration and reuse of air filter [108]. However, its electrostatic adsorption capacity still
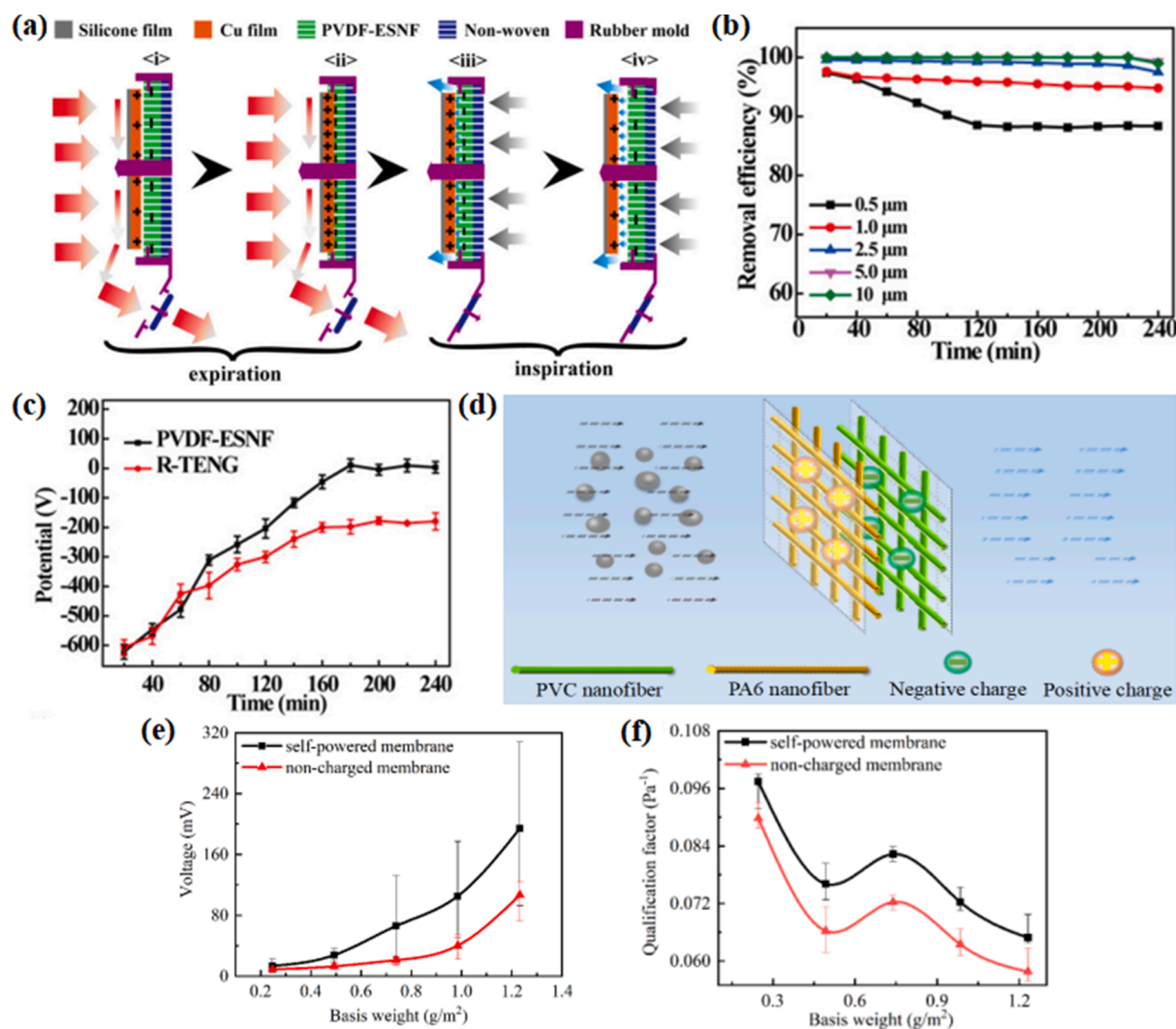
Fig. 6. (a) Working principles of the R–TENG by periodic expiration and inspiration. (b) The removal efficiency of R–TENG for particles with different diameters in 240 min durability test. (c) Average surface potential change of the single PVDF membrane and R–TENG in 240 min filtration [106]. (d) Schematic diagram for the air filtration process of the self–powered composite membrane. (e) The measured voltage on the two sides of the composite membranes of different combinations under airflow velocity of 0.1 m/s. (f) The QF of the composite membranes under airflow velocity of 0.1 m/s [107].

needs to be improved compared with electret filter. At the same time, the stability of triboelectric charge should be improved to realize long––term electrostatic adsorption.

3.1.4. Functional group interaction

Functional group interactions can be formed from unique materials with intrinsic net ions or electrons [109]. Electrospun nanofibrous air filter based on functional group interaction can achieve high–efficiency electrostatic adsorption without charging and regeneration, and is most expected to achieve long–term air filtration [57]. Bio–based polymers represented by protein and chitosan contain a large number of ionizable amino and hydroxyl groups, which are conducive to combine with negatively charged particles in the air, and enhance the filtration performance based on electrostatic adsorption [26,110–113]. More importantly, these polymers contain a large number of fully biodegradable functional groups, which can greatly reduce our dependence on fossil energy and is instrumental in environmental protection [114]. Fu et al. fabricated zein blended gelatin electrospun nanofibrous membrane realized good filtration performance of $PM_{0.3}$ (i.e., particles with diameter $\leq$ 0.3 μm) with a filtration efficiency of 98.8 % under the extremely low pressure drop of 38 Pa [115]. Zhang et al. demonstrated the possible contribution of ionizable groups to air filtration by studying the electrostatic potential on molecular van der Waals surface [116]. However, the content of bio–based polymers still needs to be well regulated to achieve stronger electrostatic adsorption [111].

In addition, inorganic matters containing ionizable ions and groups represented by metal organic frameworks (MOFs) and graphene oxide (GO) are another way to realize functional group interaction [66,117–121]. MOF is composed of metal containing nodes (ions or clusters) and organic connectors, which contain a large number of ionizable metal ions for electrostatic adsorption [122]. Guo et al. prepared an electrospun polyacrylic acid @zeolitic imidazolate framework–8 (PAA@ZIF–8), where the positive charge of ZIF–8 improved the adsorption of particles. The filtration efficiency of $PM_{2.5}$ was 99.6 %, the pressure drop was 146.3 Pa, and the QF was 0.034 Pa^{-1}, which is higher than that of commercial glass fiber [123]. Unfortunately, fragility and complex preparation are the fatal disadvantages of MOFs [57]. GO has rich functional groups and is easy to prepare with lower cost [66]. Li et al. designed GO/PAN electrospun membrane and achieved high––performance filtration of $PM_{2.5}$ owing to the rich functional groups of GO. The filtration efficiency of $PM_{2.5}$ was 99.97 % and the pressure drop was 8 Pa, which was superior to commercial filters [124]. However, these kinds of inorganic particles inevitably have the problem of easy agglomeration, which affects the uniformity of distribution. Although many crosslinkers (e.g., cellulose; PVA; PEO and PVP) [125–128] have been introduced to reduce particle agglomeration and enhance fibrous adhesion, its nanotoxicity is still debatable [79,93]. However, finding suitable materials and realizing their efficient loading are places to be explored continuously.

3.2. Function of improved slip effect

The enhanced slip effect makes the air flow pass more smoothly by optimizing the flow field, which can be realized by constructing a fluffy spatial structure and reduce the diameter of fibers.

3.2.1. Bead/Ball fibrous structure

The preparation of nanofibrous membrane containing bead or/and spherical structure filler is an effective method to increase the spacing of fibers [129–131]. By adjusting the solution parameters (i.e., surface tension; viscosity and conductivity), different forms of fibers can be prepared controllably, which can be controlled by the type and concentration of polymers [51]. The formation of bead/ball fiber in electrospinning process is closely related to the solution parameters and formed by the capillary breakup of jet [132]. In general, solutions with high surface tension will resist Coulomb forces and tend to form bead/

ball fibers; low solution viscosity cannot overcome the surface tension due to the weaker entanglement between molecular chains, so it tends to form bead/ball fibers; in addition, low conductivity systems tend to form bead/ball fibers because of insufficient Coulomb force [133–135]. Gao et al. prepared a three–dimensional (3D) PAN composite membrane with high porosity and low resistance, which was composed of scaffold nanofibers, microspheres and fine nanofibers by adjusting the solution concentration, as shown in Fig. 7(a). The microsphere enlarged the gap between the fibers, which greatly reduced the pressure drop. As shown in Fig. 7(b), the fibrous membrane with microsphere embedment (PAN–F10/S3, PAN–F10/S4, PAN–F10/S5 and PAN–F10/S6) showed uniform pore distribution, and the average flow pore diameters were 2.51, 1.46, 1.42 and 1.37 μm, respectively, which were larger than those without microsphere embedment (1.17 μm). Therefore, at the same gram weight (0.46 g/m^2), the fibrous membranes with microspheres showed lower pressure drop (109.7, 138.2, 152.7 and 164.3 Pa, respectively) than those without microspheres (filtration efficiency was 96.3 % and pressure drop was 166.1 Pa), and because the PAN–F10/S5 and PAN–F10/S6 distributed 80 nm fine fibers, ensuring higher filtration efficiency and realizing better filtration performance (QF were 0.0231 Pa^{-1} and 0.0222 Pa^{-1}, respectively) than those without microspheres (QF was 0.0185 Pa^{-1}), as shown in Fig. 7(c). Finally, fibrous membrane with microspheres showed a low pressure drop (126.7 Pa) for NaCl aerosol particles while maintaining a high filtration efficiency (99.99 %), which was much better than commercial glass fiber and melt–blown PP filter [136]. Recently, simulation technology has also been used to prove the feasibility of bead/ball structure to improve filtration performance. Yousefi et al. proposed a physics–based modeling technique to simulate the 3D microstructure of electrospun filter with embedded spacer particles. The pure fibrous medium was much thinner and the density was much higher compared with the particle embedded one with the same basis weight so that the increased pressure was much greater than the improved filtration efficiency. Thus, adding spacer particles helped to improve the QF of the filter [137]. Bead/ball fibers are spontaneously formed in–situ during electrospinning, which is a simple method. Nevertheless, the density of bead/ball fiber should be further adjusted to achieve better filtration performance. In addition, because the formation of bead/ball fiber is very limited by the solution parameters, it may be inhibited when additional solution components are added, which is not conducive to the preparation of multifunctional fibrous membrane [131].

3.2.2. Crimped fibrous structure

The preparation of crimped fiber is another effective method to increase the fluffy degree and achieve high porosity, which is relying on its unique spatial supporting. Li et al. reported a biomimetic and one–step strategy to fabricate ultrafine and crimped wool–like PVDF nanofibrous membrane, achieving high–performance air filtration. The key of preparation was to control the exchange rate between water and solvent molecules during jets flight. The charged jet will experience the bending disturbance driven by Coulomb repulsion. The premature solidification of the jet caused by water will promote the preparation of crimped fibers. Finally, the porosity of that membrane was as high as 98.7 %, which had never been achieved by one–step electrospinning. The filtration efficiency was 99.952 %, resistance less than 0.05 % of atmospheric pressure, and the QF was 0.15 Pa^{-1}, which was higher than that of commercial melt–blown filter [89]. On this basis, our research group further proved the contribution of crimped fibers to the enhanced slip effect by simulating the air flow field around spiral fibers. The pressure distribution between the layers of spiral nanofibers was more uniform (Fig. 7(d)) than that of cylindrical fibers (Fig. 7(e)), showing a uniformly distributed low pressure. In addition, due to the existence of hollow gap in the spiral fiber, the air flow tended to be evenly distributed and the flow velocity decreased, as shown in Fig. 7(f) and (g). Therefore, the crimped fibers can enhance the slip effect through the optimized flow field. Ultimately, the QF of the prepared curled PVDF
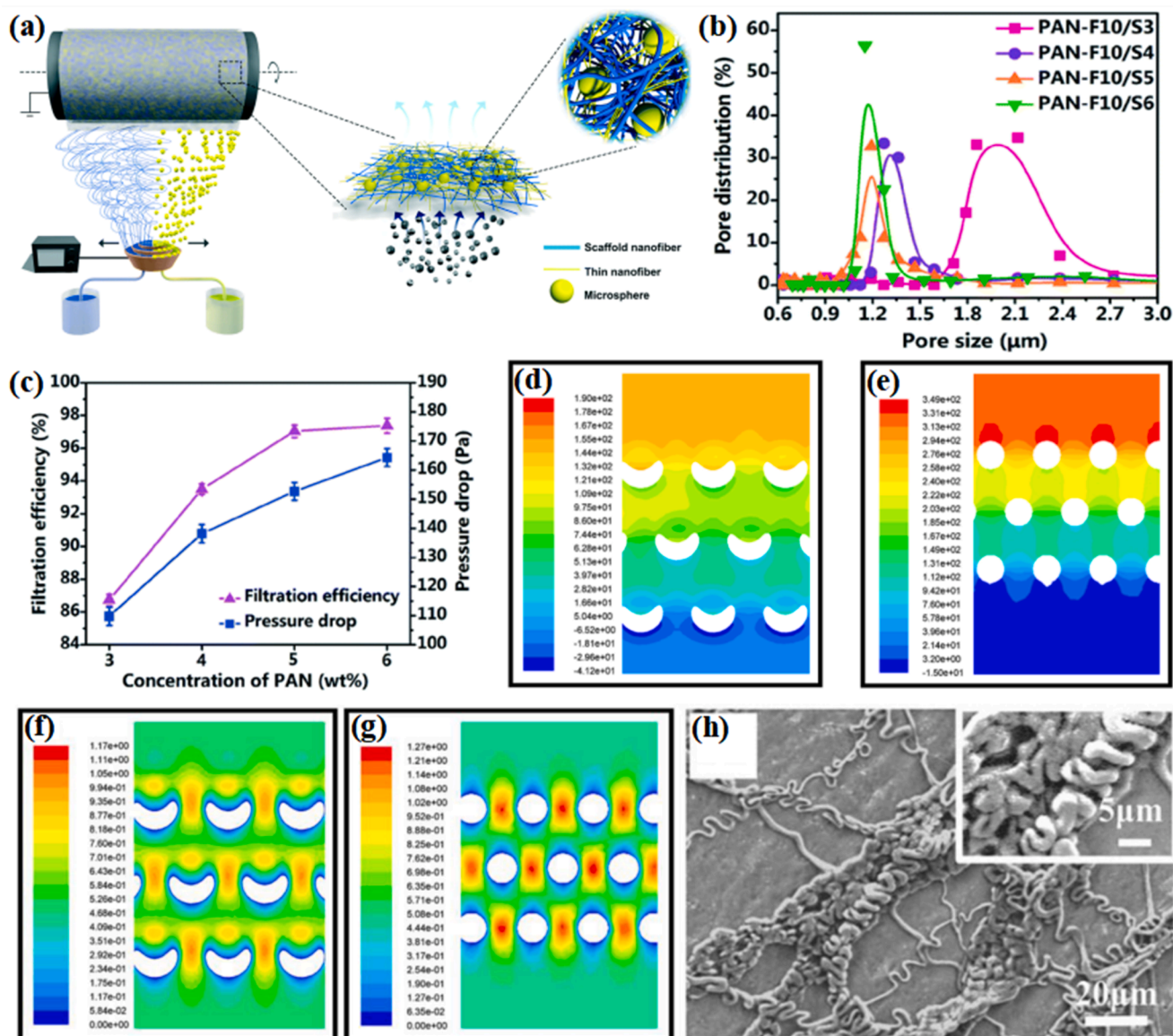
Fig. 7. (a) Preparation process of PAN three–dimensional composite membrane and its structure. (b) Pore size distribution; (c) filtration efficiency and pressure drop of PAN nanofibrous membrane containing microspheres [136]. The static pressure distributions of the airflow inside: (d) spiral fibers and (e) straight fibers. The velocity distributions of the airflow inside: (f) spiral fibers and (g) straight fibers. (h) The SEM image of spiral PVDF fibers [138].

nanofibers (Fig. 7(h)) was 12.77 % higher (0.0309 Pa^{-1}) than that of straight one (0.0274 Pa^{-1}) [138]. The preparation process of crimped fiber is relatively simple. However, the preparation conditions are relatively harsh, which limits its further development.

3.2.3. Bimodal fibrous structure

Bimodal fibrous structure refers to the complex of two fibers with significantly different diameters, where coarse fibers are used as supporting skeleton to reduce pressure drop, and fine fibers are used as the main filtration layer [29,70,139].

Multi–jet electrospinning is the most common method to construct bimodal structure, which is prepared by electrospinning layer by layer or co–electrospinning with different diameters of fibers [70,115,140]. Wang et al. designed a bimodal poly(lactic acid) (PLA) fibrous membrane with micron diameter (PLA–P) and nano diameter (PLA–N), as shown in Fig. 8(a). The filtration performance of PLA bimodal structure (mass ratios of PLA–N: PLA–P = 1: 5) was better (QF up to 0.0299 Pa^{-1}) than that when they were used alone (QFs only PLA–N and only PLA–P were 0.0276 and 0.0113 Pa^{-1}, respectively), as shown in Fig. 8(b).

Moreover, they proved that the bimodal filter with double–layer structure (DSM) has better filtration performance than the interlaced structure (ISM) due to the compensation of the inferior parts. The QF of ISM was 0.0299 Pa^{-1} and that of DSM was 0.0303 Pa^{-1}, and all of them were better than that of commercial HEPA [141]. Our group fabricated PVDF/PAN bimodal nanofibrous membrane, and also proved that the composite method of electrospinning layer by layer has better filtration performance than co–electrospinning: the QF of the former was 0.0376 Pa^{-1} and that of the latter was 0.0365 Pa^{-1} under the same basis weight. Furthermore, increasing the proportion of coarse PVDF fibers in bimodal membrane with double–layer structure would further improve the filtration performance, because too many fine PAN fibers would make the pressure drop rise sharply, and the adverse impact exceeded the contribution of improved filtration efficiency to performance. Finally, the QF of the optimized bimodal fibrous membrane was 0.0398 Pa^{-1} [142]. Nevertheless, the fibrous diameter with the best slip effect of bimodal fibrous membrane remained to be explored. For this purpose, Quan et al. modeled the slip effect of a single nanofiber. The effect of nanofibrous diameter on pressure drop was numerically simulated to
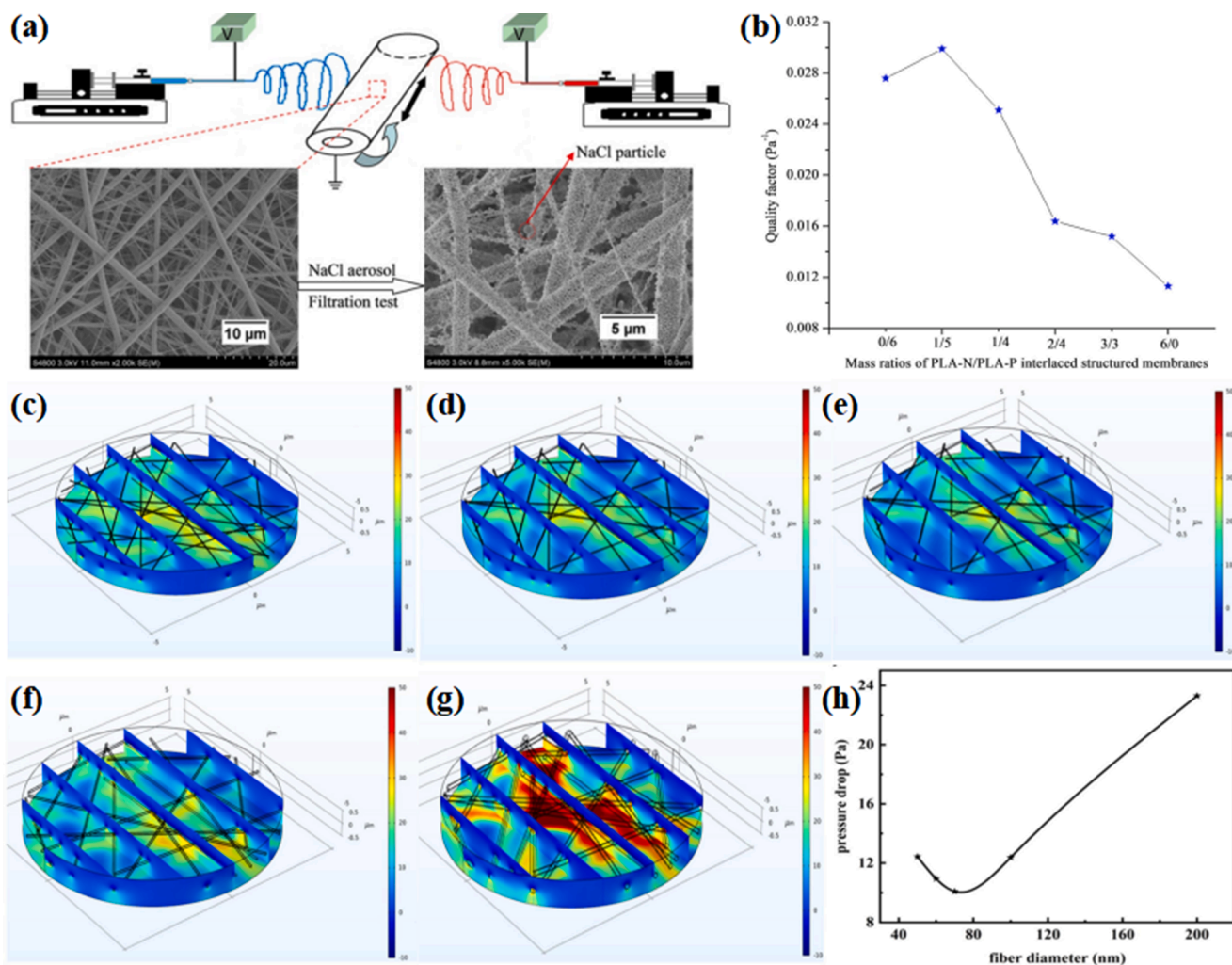
Fig. 8. (a) Preparation process of PLA bimodal membrane and its structure. (b) QF of PLA–N/PLA–P interlaced structure with different mass ratios [141]. The simulated pressure with the fiber diameters of (c) 50, (d) 60, (e) 70, (f) 100, and (g) 200 nm. (h) The pressure drops of fibrous membranes with different fiber diameters [60].

determine unimodal and single layer fiber diameter with the best slip effect under same fiber packing densities 8 %, as shown in Fig. 8(c)–(g). The pressure drop at the top remained the same, so the lighter the bottom color, the smaller the pressure drop. As the fiber diameter decreased from 200 to 70 nm, the pressure drop decreased to 10.092 Pa. However, when the fiber diameter further decreased from 70 nm to 50 nm, the pressure drop increased. This may be because the fiber diameter of 70 nm was closest to the average free path of air molecules (66 nm), as shown in Fig. 8(h). Then, the best bimodal fibers were determined (70 and 200 nm, respectively), which the filtration performance (QF = 0.065 Pa^{-1}) was better than that of unimodal fibrous filters (QF = 0.058 Pa^{-1}) [60]. Hence, the bimodal nanofibrous membrane constructed by layer–by–layer electrospinning has better filtration performance and can easily compound a variety of membranes with different functions, which is helpful to the preparation of multifunctional, efficient and low resistance fibrous membrane. However, the complex steps limit the improvement of preparation efficiency. Thus, Zhou et al. demonstrated one–step free surface electrospinning with large–scale productivity for the first time as an air filter, which was consisted of a base fabric unwinder and multiple sets of free surface electrospinning modules, and prepared PAN membranes with coarse, medium and fine fibrous composite layers. That filter showed excellent filtration efficiency (99.97 %) and low resistance (106.8 Pa). More importantly, its output was 150 times that of the traditional single–needle electrospinning [143].

Nevertheless, the complex equipment will increase the cost of preparation.

In recent years, one–step electrospinning strategies based on electrospinning/netting and jet splitting have become effective methods to prepare bimodal nanofibrous membranes, which are created by the instability of the electrospinning jets [144]. They have attracted more and more attention because of their high filtration performance, simple fabrication steps, low cost, and scalable preparation [69].

Electrospinning/netting realizes the in–situ combination of coarse skeleton fibers and ultrafine (about 20 nm) nanonets through the formation and phase separation of charged droplets in the jets [145–147]. In the early days, nanofibrous membranes prepared by electrospinning/netting technology generally had problems such as low coverage of nanonet (<30 %) and poor process controllability (i.e., the formation of nanonets was often random), which limited the improvement of their filtration performance. Recently, Ding's team proposed that the electrospinning process has two jet modes of "jet" mode and "droplet" mode, and calculated the critical thresholds of the two modes. When the charge to mass ratio (e / m) of the jet exceeds the droplet threshold, the charged droplet will be ejected together with common jets [148,149]. Generally, high conductivity of solution (by adding metal salt solution), solute differences, and extremely low humidity (<30 % RH) contribute to the generation of nanonets [150]. Nowadays, nanofiber/net membranes with 100 % nanonet coverage can be prepared controllably, which

further improves its filtration performance. Liu et el. developed an innovative in–situ electret electrospinning/netting technology to control solution phase separation and crystal phase transition of PVDF, where lithium chloride (LiCl) or tetrabutylammonium chloride (TBAC) was used to enhance the conductivity in the system and promote the formation of charged droplets, as shown in Fig. 9(a). Finally, the nanonet coverage of the prepared PVDF nanofiber/net membrane reached 100 %, and had real nano diameter, small pore size and strong electret effect, as shown in Fig. 9(b) and (c). The air filtration efficiency was 99.998 %, the pressure drop was 93 Pa and the QF was 0.11 Pa^{-1}, showing higher particle filtration performance [149].

Similarly, jet splitting can also generate bimodal structure, in which coarse and fine nanofibers exist simultaneously. Li et al. first reported a one–step simple method to prepare PVDF tree–like nanofibrous membrane based on jet splitting by adding TBAC [151]. They observed that the membrane contained trunk fibers (100 nm to 500 nm) and branch fibers (5 nm to 100 nm), as shown in Fig. 9(d) and (e), and proved that the high conductivity of the solution was the key to achieving jet splitting. In addition, they also used a high–speed camera to capture the jet splitting phenomenon in the PVDF electrospinning process: the straight stretch section of high conductivity solution jet was shorter, and some

branch jets were continuously split from the outside of the curved section and further subdivided into many branch fibers, as shown in Fig. 9 (f) and (g). When the charge density was higher than a certain threshold, the Coulomb force overcome the surface tension and formed splitting jets. Finally, the filtration efficiency of tree–like PVDF nanofibrous membrane for 0.26 μm NaCl particles was 99.999 %, and the resistance was 126.7 Pa, which was nearly to ultralow penetration air filters [152]. Balgis et al. studied the effect of polymer solution rheological properties on the formation of cellulose/PVP bimodal nanofibers for the first time. Due to the negative zeta potential, cellulose was attracted to the surface of the positively charged jet and occupies most of its surface components, which promoted the continuous and unstable jet splitting, as shown in Fig. 9(h), resulting in the formation of two sizes of nanofibers: the average diameter of coarse fibers and fine fibers were 249 and 61 nm, respectively, as shown in Fig. 9(i). On the contrary, the size distribution of the nanofibers was not affected by the negative voltage, as shown in Fig. 9(j) and (k). Ultimately, the QF of bimodal cellulose/PVP composite nanofibrous membrane synthesized by one–step electrospinning was 0.117 Pa^{-1}, which was 10 times that of commercial HEPA filters. It is worth noting that the preparation of cellulose/PVP bimodal nanofibers got rid of the decisive influence of high conductivity on jet
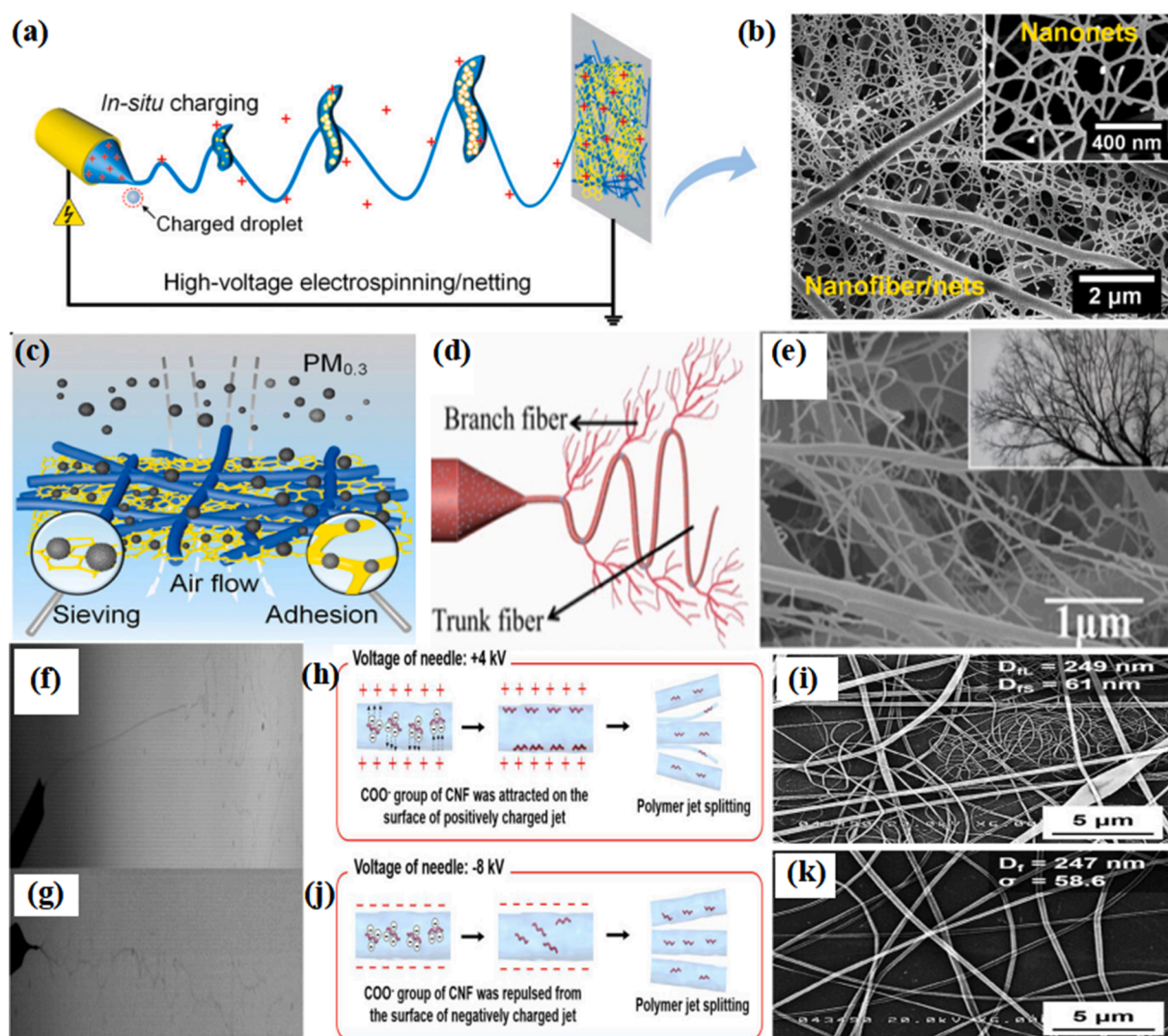
Fig. 9. (a) Schematic diagram of the electrospinning/netting. (b) SEM image of PVDF nanofiber/nets with 100% nanonet coverage. (c) Illustrating image of nanofiber/nets filtration manners [149]. (d) Schematic diagram of tree–like fibers preparation by jet splitting. (e) SEM image of tree–like PVDF nanofibers. Photo images of electrospinning jets for (f) pure PVDF solution, and (g) PVDF/TBAC solution with high conductivity[151]. (h) Extreme jet splitting model, and (i) SEM image of cellulose/PVP fibers with positive applied voltage. (j) Jet splitting model, and (k) SEM image of cellulose/PVP fibers with negative applied voltage [69].

splitting behavior: there was no component in solution that can significantly promote conductivity, but enhanced jet splitting still occurred, this provided more opportunities for jet splitting [69].

The challenge of one–step preparation of bimodal nanofibers based on jet instability lies in: realize the stable and efficient preparation under large load of various functional materials, because the splitting of jet or the phase separation of charged droplets is likely to be restrained by the introduction of functional materials (jet splitting or phase separation process will be inhibited due to high solution viscosity) [153]. Above all, it is undeniable that this simple preparation strategy has a powerful magnetizing effect on realizing the batch preparation of high performance electrospun air filter materials and promoting the electrospinning technology from laboratory to industrialization.

3.3. Function of increased contact sites

The improvement of fiber surface roughness is the key to increase the contact sites between fibers and particles, which can be realized by constructing nanofibers with different structures.

3.3.1. Porous fibrous structure

Electrospun porous nanofibers refer to the surface with a large number of nano–scale porous structures (these structures can exist only on the surface or throughout the fibers) [154]. Phase separation in electrospinning process is an important reason for the formation of porous fibers [155]. Wang et al. prepared a high filtration performance nano/porous PLA composite fibrous by adjusting the relative humidity (filtration efficiency = 99.999 %, pressure drop = 93.3 Pa). It was proved that high relative humidity will promote the formation of porous structure (Fig. 10(a)), because it allowed more water vapor in the air to cause phase separation of the jet, in which the part penetrating into the jet formed internal pores, while the part remaining on the surface of jet formed surface pores. When the humidity increased from 15 % to 60 %, the coverage of nanopores on the fiber surface increased from 1.85 % to 23.63 %, as shown in Fig. 10(b), thus, the pressure drop was decreased from 228.7 to 143.8 Pa. Although the filtration efficiency decreased, the pressure drop had decreased more, so the air filtration performance still reached the maximum when the humidity was 45 % (QF = 0.0276 Pa^{-1}), as shown in Fig. 10(c), which proved that the porous fiber could achieve high–performance air filtration [141]. Furthermore, the addition of metal–organic framework (MOF) is also easy to lead to phase separation due to the rapid evaporation of solvent [123].

Post treatment to induce phase separation of electrospun fiber is another common method to prepare porous structure. Wang et al.
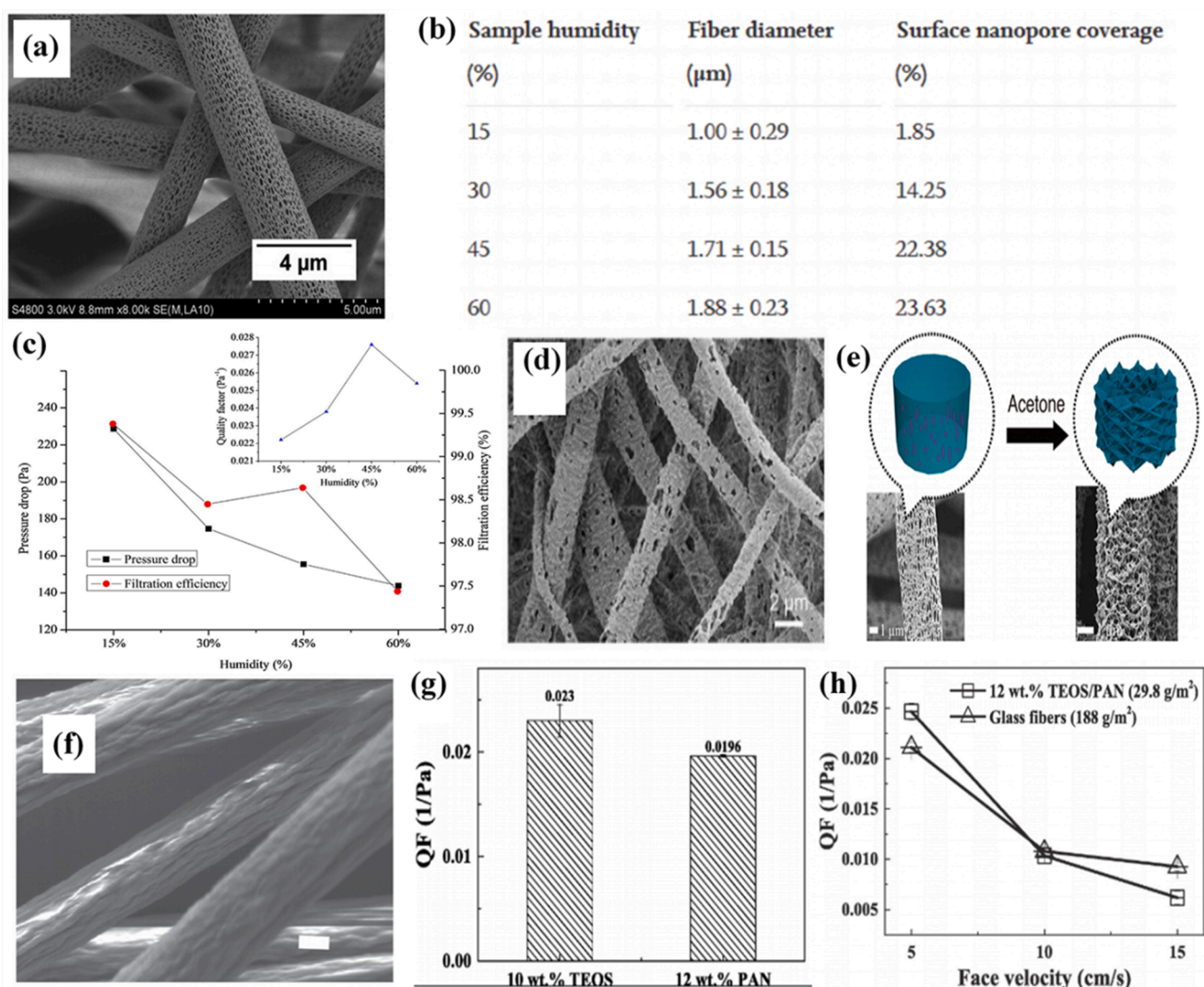
Fig. 10. (a) SEM image of PLA porous fibers. (b) Relationship between preparation humidity and fiber surface nanopore coverage. (c) Pressure drop, filtration efficiency, and QF of fibrous membrane fabricated with different humidity [141]. (d) SEM image of ultrafine PTFE porous fibers [90]. (e) SEM image of PLLA porous fibers before and after ethanol treatment [154]. (f) SEM image of PAN fold fibers. QFs of: (g) 10 wt% TEOS and 12 wt% PAN membrane, and (h) 12 wt% TEOS/PAN and glass fibers [74].

fabricated ultrafine PTFE porous fibrous membrane (Fig. 10(d)) with high filtration performance by high temperature and ethanol immersion post–treatment (filtration efficiency = 99.72 %, pressure drop = 89.9 Pa). At a high temperature of 360 ℃, PVP and PTFE melt together, and then PVP was removed with ethanol to form a PTFE porous fibers [90]. Song et al. used ethanol to induce poly(L–lactic acid) (PLLA) recrystallization to form porous fibers, as shown in Fig. 10(e). With the movement of PLLA molecular chain during crystallization, the solvent was extruded from the crystalline part of the fiber and phase separation occurred. The filtration efficiency of the prepared PLLA porous fiber for 30–100 nm NaCl particles exceeded 99.9 %, the pressure drop was 110 Pa, and the QF was 0.05–0.75 Pa^{-1}, better than commercial non–woven filter [154].

Although there is no consensus on the effect of porous fiber surface on air flow [156], it is certain that the rough surface of porous fiber will increase the friction coefficient between fiber and particles, which is conducive to particle capture and thus improving the filtration performance [141].

3.3.2. Fold fibrous structure

The folded fiber morphology is caused by buckling instability [131].

Different evaporation rates of mixed solvents are one of the reasons for the formation of fold fibers. Attabi et al. dissolved PAN with tetraethyl orthosilicate (TEOS) and $N—N$ dimethylformamide (DMF) to prepare fold PAN fibers (Fig. 10(f)). The different evaporation rates of TEOS and DMF will cause phase separation, resulting in fiber folding. This fold surface would increase the specific area of nanofibers, thus increasing the surface area of adsorption and capture for particles. In addition, it could also hinder the movement of particles in the air flow, or expand the anti–skid surface and the stagnation area of the fiber surface, so as to improve the adhesion between particles and the surface of fiber, which will greatly improve the capture ability of large particles. With the increase of fiber surface roughness, the filtration performance will also increase. The filtration performance of fold PAN fibrous membrane (i.e., 10 wt% TEOS, QF = 0.023 Pa^{-1}) was better than that of smooth one (i.e., 12 wt% PAN, QF = 0.0196 Pa^{-1}) and glass fiber commercial filter (QF = 0.021 Pa^{-1}), as shown in Fig. 10(g),(h) [74].

Removing or migrating some components from fibers by post––treatment is another effective method to construct fold nanofibers. Fan et al. treated polyimide (PI) / PAN composite fiber membrane at high temperature of 480 ℃ to remove PAN, and then PI fold nanofibers were formed, as shown in Fig. 11(a). Particles will reflect and escape on the
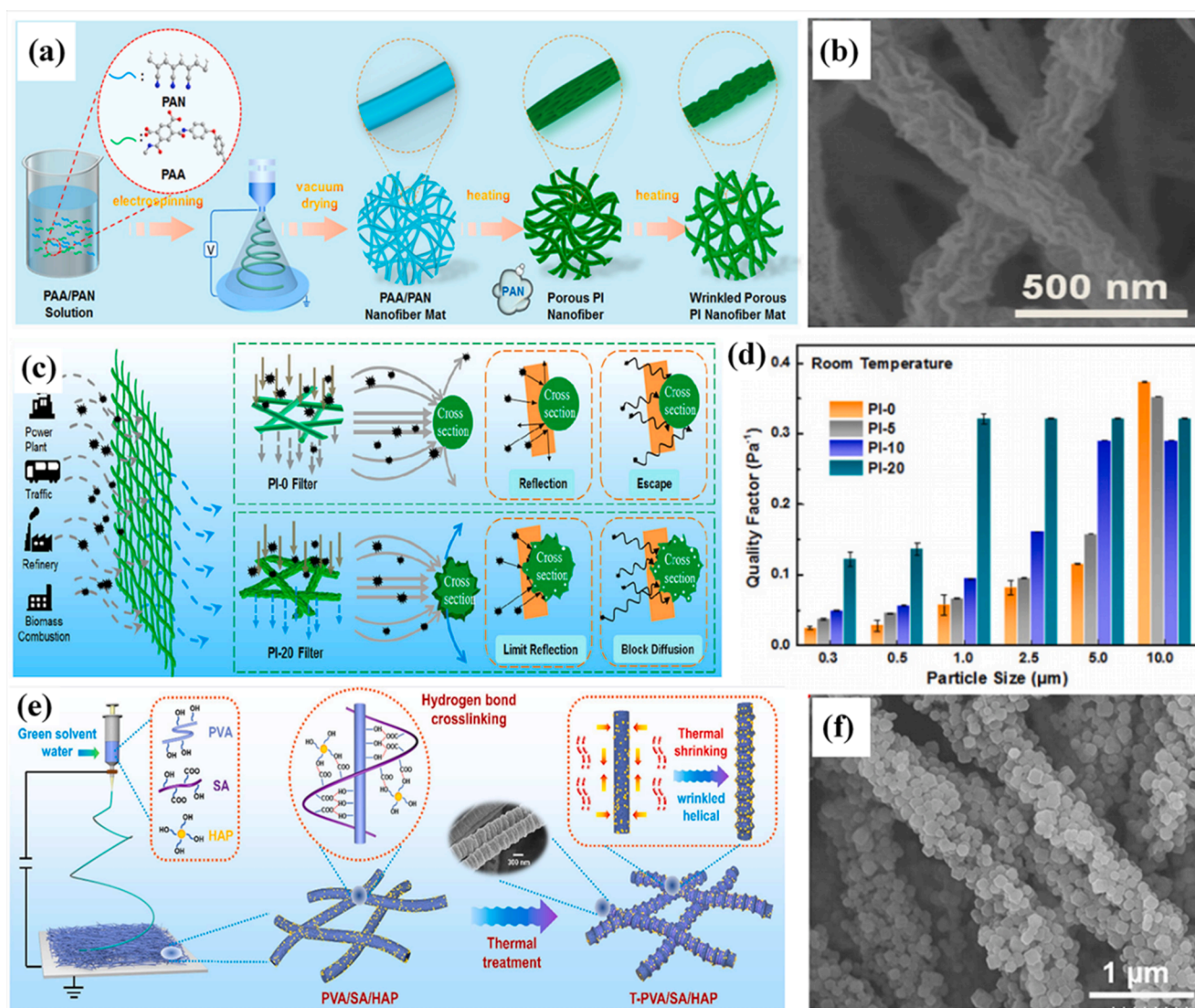
Fig. 11. (a) Schematic illustration for fabrication of the wrinkled PI nanofibers. (b) SEM image of the wrinkled PI nanofibers. (c) Schematic illustration for filtration mechanism of wrinkled filter. (d) QFs of different PI membranes for filtering different diameter particles under room temperature [155]. (e) Schematic illustration for fabrication of the T–PVA/SA/HAP nanofibers [157]. (f) Micromorphology of PI–POSS@ZIF fibers with nanoprotrusions [158].

smooth fiber surface (PI–0); in contrast, nanofibers with rough surface (PI–20, Fig. 11(b)) will greatly limit the elastic reflection of particles and "stick" to the fiber surface directly or through reflection, which was not easy to fall off due to inertia, as shown in Fig. 11(c). Finally, the filtration efficiency of fold PI fibrous membrane for $PM_{0.3}$ was 99.99 %, the pressure drop was only 43.25 Pa, and the QF was as high as 0.1228 Pa^{-1}, which was 3.93 times that of smooth PI fibrous membrane (0.0249 Pa^{-1}), as shown in Fig. 11(d) [155]. Similarly, Deng et al. prepared polyvinyl alcohol/sodium alginate/hydroxyapatite (T–PVA/SA/HAP) electrospun nanofibers with a unique wrinkled helical structure by green electrospinning and thermal treatment, as shown in Fig. 11(e). The activation of PVA/SA polymer chain and the migration of HAP particles was promoted, and realized the regeneration of hierarchical structure, which increased the contact area between fibers and particles, thus improved the filtration performance. The filtration efficiency for 0.3–2.5 μm particles was 99 %, and the pressure drop was 96.32 Pa [157]. Similar to porous fibers, the influence of fold fibers on air fluid has not been determined, but its contribution to the improvement of air filtration performance cannot be erased.

3.3.3. Nanoprotrusion fibrous structure

Forming a large number of nanoprotrusions on fibers is an effective way to increase the surface roughness of fibers, which can be fabricated by particle doping through hydrogen bond or coordination bond, such as MOFs, GO, zinc oxide (ZnO), SiO_2, protein particles and so on [40,139,158,159]. It is desirable to construct uniform and widely distributed nanoprotrusion [14]. However, particle agglomeration is inevitable. In order to solve this problem, a variety of methods have been studied, including introducing dispersant, ultrasonic vibration for a certain time, coaxial electrospinning, etc., all of which have achieved good results [14,160]. Nevertheless, there is often a problem of particle desorption caused by insufficient adhesion between nanoprotrusions and smooth fibers. Therefore, Xie et al. added octa(amino--propylsilsesquioxane) (POSS–NH_2) as a bridge to anchor ZIF–8 particles on PI fibers, and prepared PI fibrous membrane (PI–POSS@ZIF) with a large number of uniformly distributed nanoprotrusions, as shown in Fig. 11(f). POSS can enhance the binding energy of the interface, so that ZIF–8 was more firmly attached to the smooth fiber. The removal rate for $PM_{0.3}$ was up to 99.28 %, the pressure drop was 49.21 Pa, and the QF was 0.1002 Pa^{-1} [158].

Indeed, the contribution of nanofibers with nanoprotrusion structure to air filtration often comes more from the inherent function of the introduced particle itself, the ability of nanoprotrusion fiber with rough surface to particle filtration should not be ignored, as the same to fold structure.

4. Design of multifunctional electrospun air filter

Nowadays, as people pay more and more attention to personal protection, the use frequency of air filter is getting higher and higher, and a single high filtration performance can no longer meet the demand: more attention has been paid to how to maximize the benefits of personal protection and optimize the feeling of use [5,13,14]. The introduction of functional materials and the design of special structures are common methods for endowing electrospun air filter with various performances: all this is based on the premise of meeting the high filtration capacity of the air filter.

4.1. High dust holding capacity

Dust holding capacity refers to the mass of particles that can be captured when the pressure drop reaches twice the initial value, which may affect the comfort of user [4]. In the process of use, particles will continuously deposit on the surface or inside of the air filter, thus affecting the air circulation [161]. Therefore, large dust holding capacity can ensure comfortable personal protection for a long time, and it

is no need to worry about changing filter in hazardous environments [44]. Generally, the dust holding capacity of filter relying on surface filtration is relatively small, while that depending on deep filtration is greater, because the former is easy to cause blockage, the pressure drop rises sharply; the latter relies on tortuous three–dimensional channels, and it is not easy to jam [95]. Thus, designing the structure of air filter to achieve better deep filtration is the key to improve the dust holding capacity [162]. Gradient structure is an effective method to realize deep filtration. Zhang et al. firstly reported a polysulfone (PSU)/PAN/PA–6 electrospun air filter with gradient reduced fiber diameter (1 μm/200 nm/20 nm) to realize durable and efficient filtration (filtration efficiency for 0.3 μm NaCl particles was 99.992 % and pressure drop was 118 Pa). PSU, PAN and PA–6 membranes with different pore sizes are respectively responsible for hierarchical filtration of large, medium and small diameter particles, respectively, as shown in Fig. 12(a), realizing the effect that one plus one is greater than two: higher filtration efficiency with minimal pressure drop was achieved [67]. Next, Chen et al. prepared TPU / PS / PA6 composite membrane with multilevel structure (Fig. 12(b)) and evaluated its service life for the first time (filtration efficiency for 0.3 μm NaCl particles was 99.99 % and pressure drop was 54 Pa). They found that the service life of the composite membrane was better (15 min) when the larger diameter TPU was located upstream and the smallest diameter PA6 was located downstream (10PA–6/60PS/30TPU); while the service life was worse (9 min) when PA6 was located upstream and TPU was located downstream (30TPU/60PS/10PA–6), as shown in Fig. 12(c). For the latter, the PA6 layer in the upstream was closely stacked, and the dust cake was easier to form on the surface and significantly increased the pressure drop; the former had a larger cavity structure, which was conducive to the transportation of particles in the membrane and was not easy to be blocked, so as to improve the service life. Moreover, when the electrospinning time of the PS layer was increased from 30 to 90 min, the service life was improved from about 6 min to about 13 min, which was attributed to the larger cavity structure, as shown in Fig. 12(d) [68].

Afterwards, Su et al. fabricated multilayer poly(arylene sulfide sulfone) (M–PASS) electrospun nanofibrous membrane with coarse fibers (C–PASS), fine fibers (F–PASS) and bead fibers (B–PASS), as shown in Fig. 12(e) (filtration efficiency for 0.3–2.5 μm particles was 99.97 % and pressure drop was 44.3 Pa), which further proved the contribution of enlarged cavity structure to the improvement of dust holding capacity. The PASS fiber with bead structure had the highest dust holding capacity (24.7 ± 0.6 g/m^2) compared with other straight PASS fibers (17.1 ± 0.2 and 18.1 ± 0.4 g/m^2) because the existence of bead like structure enlarged the cavity structure in the fibrous membrane and the space between fibers; the dust holding capacity was related to the porosity of the fibrous membrane: the higher the porosity, the better the dust holding capacity, as shown in Fig. 12(f) [163]. The preparation of high dust holding capacity fibers by simplified steps is the goal to be explored in the future.

4.2. Water vapor transfer

During the use of the air filter, the exhaled water vapor may cause uncomfortable feelings: for hydrophobic materials, low water vapor transmission rate will lead to a sense of moisture, while for hydrophilic materials, the moisture will be absorbed to form a liquid film and make the air resistance rise rapidly. The purpose of water vapor transmission system is to achieve efficient directional transmission of water droplet and vapor, thus avoid the rising air resistance and wet–sticky feeling caused by exhaled water vapor to realize comfortable use [164]. Constructing hydrophobic/hydrophilic gradient structure (i.e., Janus membrane) is an effective method to realize directional water droplet or vapor transport, which has been widely used in wound dressing, protective clothing, oil–water separation and so on [165–168]. Water vapor will spontaneously transfer from hydrophobic surface to hydrophilic surface due to different wettabilities [169]. Zhao et al. prepared air filter
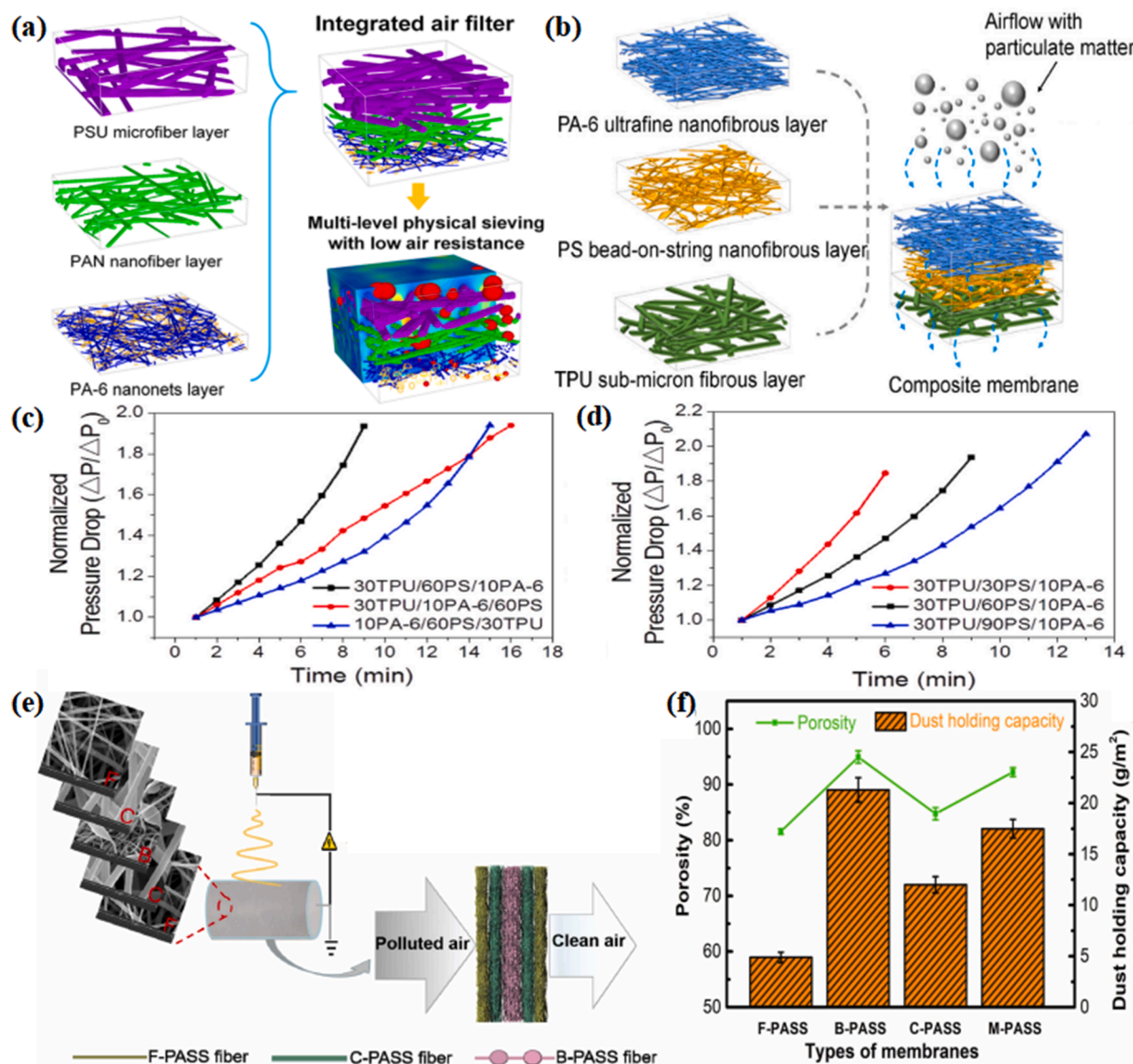
Fig. 12. (a) Schematic illustration for structure of multilevel PSU/PAN/PA–6 membrane [67]. (b) Schematic illustration for structure of TPU/PS/PA–6 composite membrane. (c), (d) Service times of different composite membranes [68]. (e) Fabrication process of M−PASS nanofibrous membrane. (f) Porosity and dust holding capacity of different nanofibrous membranes [163].

with water vapor transfer function for the first time, which was composed of hydrophobic PVDF nanofibers, PVDF/PAN contained SiO_2 (PAN–SiO_2) composite nanofibers, and super–hydrophilic PAN–SiO_2 nanofibers, as shown in Fig. 13(a). High dipole moment and fine diameter of PAN fibers greatly increased air filtration performance (filtration efficiency for $PM_{2.5}$ was 99.99 % and pressure drop was 86 Pa). They found that the strong hydrophilicity of nanomaterials would accelerate the adsorption–desorption process of water molecules, as shown in Fig. 13(b), so as to improve the evaporation rate, and the fine fiber diameter also promoted water evaporation due to an enlargement of the surface area, as shown in Fig. 13(c), the finer the diameter, the higher the water evaporation rate. Furthermore, the membrane with gradient structure (from hydrophobic to hydrophilic) could effectively transport water vapor: the vapor transmission time from hydrophobic side to hydrophilic side (30 min, M2) was much shorter than that from hydrophilic side to hydrophobic side (47 min, M1), as shown in Fig. 13 (d). Finally, the water vapor transmission rate of the prepared PVDF/PAN nanofibrous membrane was 13.612 $gm^{-2}d^{-1}$, which was better than the commercial samples (about 10.8 $gm^{-2}d^{-1}$) under the same pressure drop [170].

Subsequently, more and more scholars have prepared air filter with better filtration performance and water vapor or water droplet transportation [164,171,172]. However, the mechanism of water vapor directional transport has not been well explained; the influence of hydrophilic/hydrophobic layer thickness on water vapor transmission effect has not been deeply explored; and the stability of hydrophilic/hydrophobic structure needs to be improved (e.g., in the process of use, the composite layer is inevitably prone to delamination, which will affect water transport) [167].

4.3. Antibacterial activity

Particles in the air often contain a large number of bacteria, which will pose potential risks to human health [6,31,173]. Therefore, the endowment of antibacterial properties of air filters has become a research hotspot, which can prevent people from being injured by bacteria [32,174,175]. At present, most antibacterial materials are mainly based on the adsorption and lysis of cations on the negatively charged cell membrane and cell wall of bacteria, such as nanoparticles of metals and their oxides (TiO_2, silver (Ag), ZnO, SiO_2, MOFs), and some
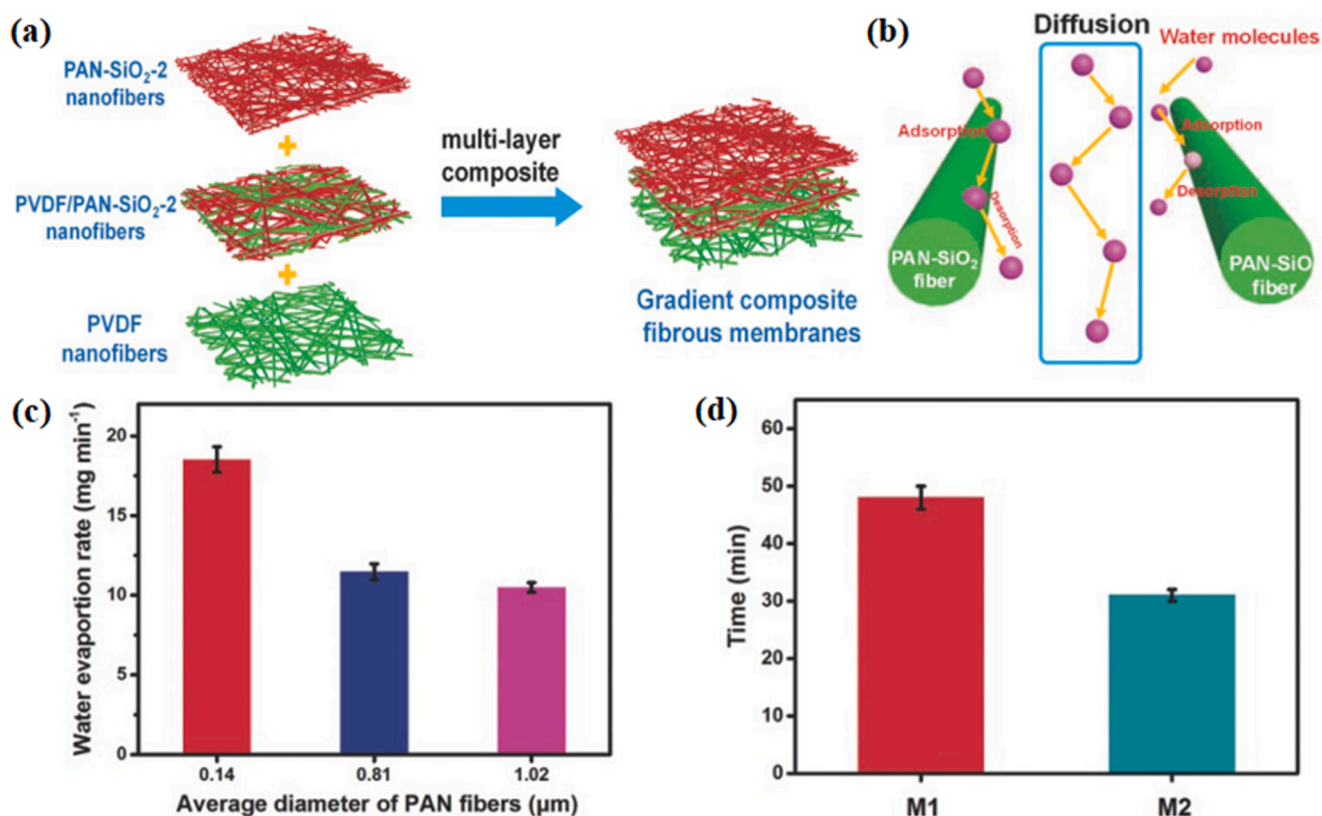
Fig. 13. (a) Schematic illustration for the fabrication process of gradient composite fibrous membranes. (b) Mechanism of transferring water molecules. (c) Water evaporation rate of PAN fibers with different diameters. (d) Time of increase of the humidity from 40% to stable value with different membranes [170].

polymers (chitosan (CS) and *N*–halamine) [6,31,32,173–176]. In addition, the polymers which extracted from some natural herbs have also been proved to achieve antibacterial function by targeting specific groups of bacteria, such as sophora flavescens and curcumin (Cur) [177–179]. In contrast, metal and its oxide nanoparticles have better antibacterial properties because of their easier ionization characteristics. Xiao et al. prepared tree–like bimodal PVDF nanofibers containing silver nanoparticles, as shown in Fig. 14(a), with antibacterial rates of more than 99.6 % against *Staphylococcus aureus* and *Escherichia coli*, and high filtration performance (filtration efficiency was 99.95 %–99.97 % and pressure drop was 137.5 Pa) [180]. Nevertheless, the introduction of nanoparticles may bring nanotoxicity. Although Li et al. have proved that their TiO_2 nanoparticles can adhere to fibers stably, further clinical experiments were still needed to verify the safety [173]. In short, the potential nanotoxicity limits the further application of nanoparticles in antibacterial personal protection. Constructing all–polymer nanofibrous membrane is a good strategy to avoid nanotoxicity. Zhang et al. fabricated multilayer bimodal nanofibrous membrane composed of PVA, CS and *N*–halamine (PVA/CS/*N*–halamine), as shown in Fig. 14(b), which showed an obvious inhibitory region against *Escherichia coli* and *Staphylococcus aureus*, and relatively good air filtration performance (filtration efficiency for 300–500 nm NaCl particles was 99.3 %, pressure drop was 183 Pa, and QF was 0.027 Pa^{-1}, as shown in Fig. 14(c)) [176]. However, such filtration performance is hard to be satisfactory because the introduction of natural antibacterial agents will often limit electrospinnability and decrease filtration performance. To this end, based on PA6 / PVP system with low binding energy, our group introduced CS and Cur to realize enhanced jet splitting and efficient loading of antibacterial agents, as shown in Fig. 14(d), preparing bimodal nanofibers loaded with a large number of ultrafine nanofibers (PA6/PVP@CS@Cur), as shown in Fig. 14(e), and realizing higher performance air filtration (filtration efficiency for 0.3 μm NaCl particles was 99.83 %, pressure drop was 54 Pa, and QF was 0.118 Pa^{-1}), which showed more stable

filtering performance than commercial masks: the filtration efficiency of PA6/PVP@CS@Cur membrane decreased from 99.84 % to about 99 %, while that of commercial mask decreased from 98 % to 92 %, as shown in Fig. 14(f). The synergistic effect of CS and Cur further promoted the antibacterial properties (antibacterial activities against *Escherichia coli* and *Staphylococcus aureus* were 99.5 % and 98.9 %, as shown in Fig. 14 (g)) [153]. However, the introduction of natural antibacterial agents into electrospinning air filter is still challenging, and more strategies should be developed to meet the diversified preparation of antibacterial high–performance air filter.

4.4. Gaseous pollutants absorption

Gaseous pollutants are pollutants that exist in molecular state under normal conditions, such as sulfur oxides, nitrogen oxides and VOCs [118]. Most of them have uncomfortable smell, toxicity, irritation, teratogenicity and carcinogenicity, which will cause great harm to human health [181]. Endowing the air filter with gaseous pollutants adsorption capacity will prevent the human body from being harmed by VOCs. However, general commercial masks have little adsorption capacity for gaseous pollutants, and ordinary electrospun nanofibers are also powerless because there is almost no interaction between them and gas molecules [182]. The introduction of components that can interact with gas pollutant molecules into electrospun fibers will greatly improve the gaseous pollutants adsorption capacity of the prepared filter, such as activated carbon, β–cyclodextrin (β–CD), gelatin and MOFs [181,182]. The high specific surface area of adsorbents and exposure to gas as much as possible are the key to improve the gaseous pollutants adsorption capacity. MOF is a kind of crystalline porous materials with periodic network structure formed by self–assembly between metal ions or clusters and organic ligands. It is famous for high specific surface area and is widely used for VOC adsorption [118]. Hu et al. prepared ZIF–67 loaded graded porous PS nanofibrous membrane, in which ZIF–67
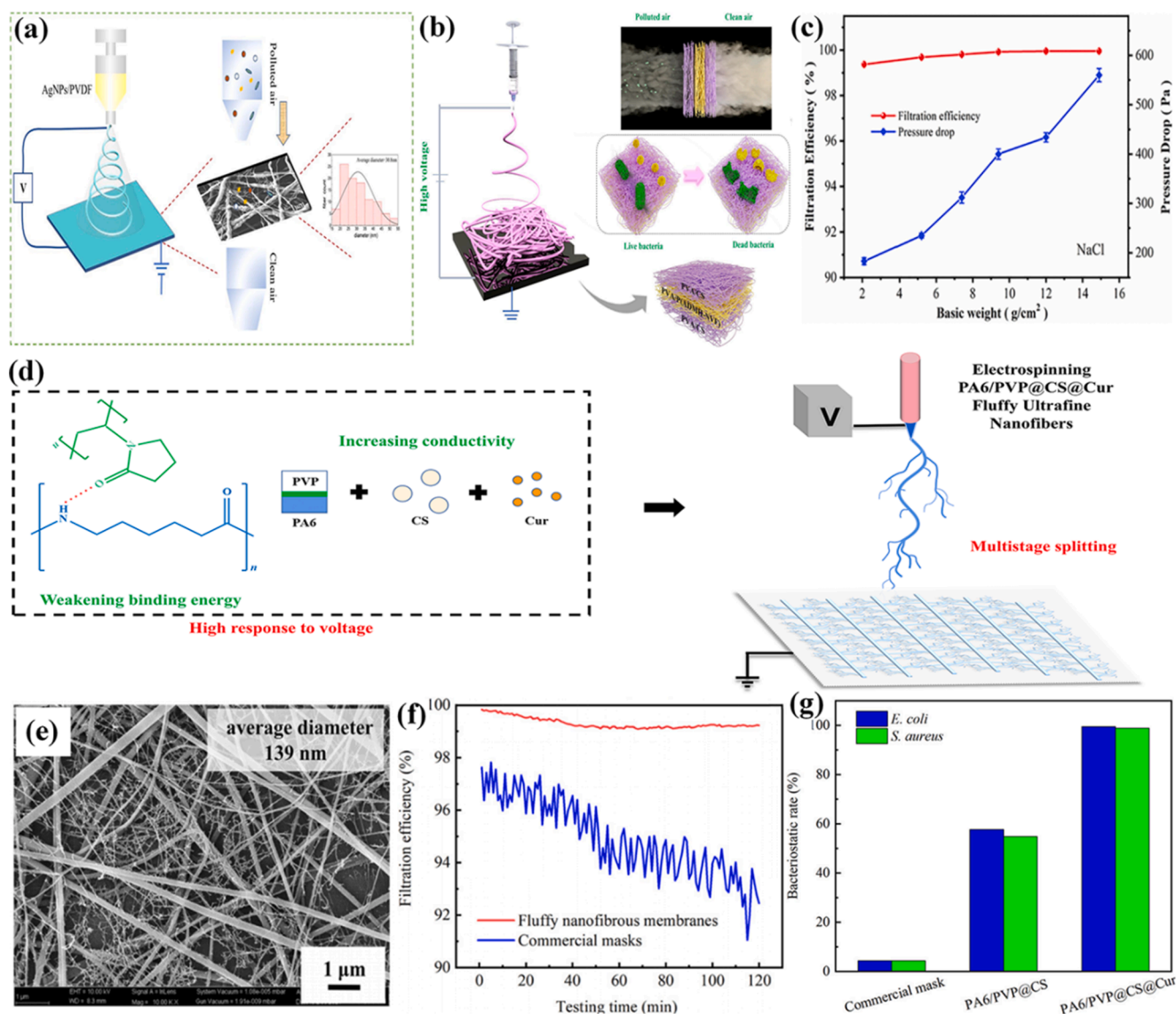
Fig. 14. Schematic illustration for the fabrication process of (a) tree–like bimodal PVDF nanofibers containing silver nanoparticles [180]; (b) multilayer bimodal PVA/CS/*N*–halamine membrane [176]. (c) Filtration efficiency and pressure drop of PVA/CS/*N*–halamine membrane with different basic weights [176]. (d) PA6/PVP@CS@Cur ultrafine nanofibers. (e) SEM image of PA6/PVP@CS@Cur nanofibers. (f) Filtration efficiency of fluffy nanofibrous membranes and commercial masks under 120 min filtering test. (g) Antibacterial rates of different membranes against *Escherichia coli* and *Staphylococcus aureus* [153].

aimed to create interconnected mesoporous and macroporous structures, as shown in Fig. 15(a), promoting SO_2 exposure to the pores of ZIF–67, thereby enhancing adsorption performance, as shown in Fig. 15 (b). The excellent SO_2 adsorption capacity of 1362 mg/g was achieved at room temperature and 55 % RH. In addition, the introduction of ZIF–67 enhanced the electrostatic adsorption and achieved efficient filtration performance: filtration efficiency for 0.3 μm particles was 99.921 % and pressure drop was 91 Pa [183]. Nevertheless, electrospun fibers usually have smooth surfaces and lack active groups, which makes it difficult to anchor MOFs. For this reason, Fan et al. focused on strengthening the interface structure and manufactured PI hybrid filter through multiple hydrogen bond self–assembly: octa(amino–propylsilsesquioxane) (POSS–NH_2) was used as a bridge to anchor amino–functionalized zeolitic imidazolate framework–8 (NH_2–ZIF–8) and PI fibers, as shown in Fig. 15(c). Thus, the stable load of ZIF–8 was realized: the grafted particles on the fiber surface did not fall off after purging the prepared fiber membrane with a manually made nitrogen purging device for 60 min. After loading ZIF–8 with enhanced hydrogen bond (PI–POSS@ZIF), the adsorption capacities of formaldehyde, benzene, toluene and aniline

were 89.95, 245.31, 185.68 and 207.49 mg/g, respectively, improved significantly, as shown in Fig. 15(d). The enhanced electrostatic effect of ZIF–8 also improves the filtration performance (filtration efficiency for $PM_{0.3}$ was 99.28 % and pressure drop was 49.21 Pa) [158]. However, the preparation of MOF is complex and it is easy to agglomerate; more importantly, the introduction of MOF will inevitably bring nanotoxicity, which will also limit its further use for personal protection.

β–CD is a low–cost cyclic oligosaccharide with conical structure, which can capture a variety of gas molecules, such as formaldehyde, aniline and styrene [184]. By mixing with traditional electrospun polymers, all–polymer β–CD nanofibrous membrane can be prepared, which can avoid nanotoxicity. The drawback is that the adsorption performance of β–CD alone for VOC is insufficient. Thus, Kadam et al. electrospun geltain/β–CD nanofibrous membrane to improve the adsorption capacity of VOCs, as shown in Fig. 15(e). Gelatin was a low–cost and widely available protein biopolymer with many functional groups. Composite geltain/β–CD nanofibrous membrane would exert their respective functional groups to enhance VOCs adsorption capacity: it had excellent adsorption properties for p–xylene (287 mg/g), benzene
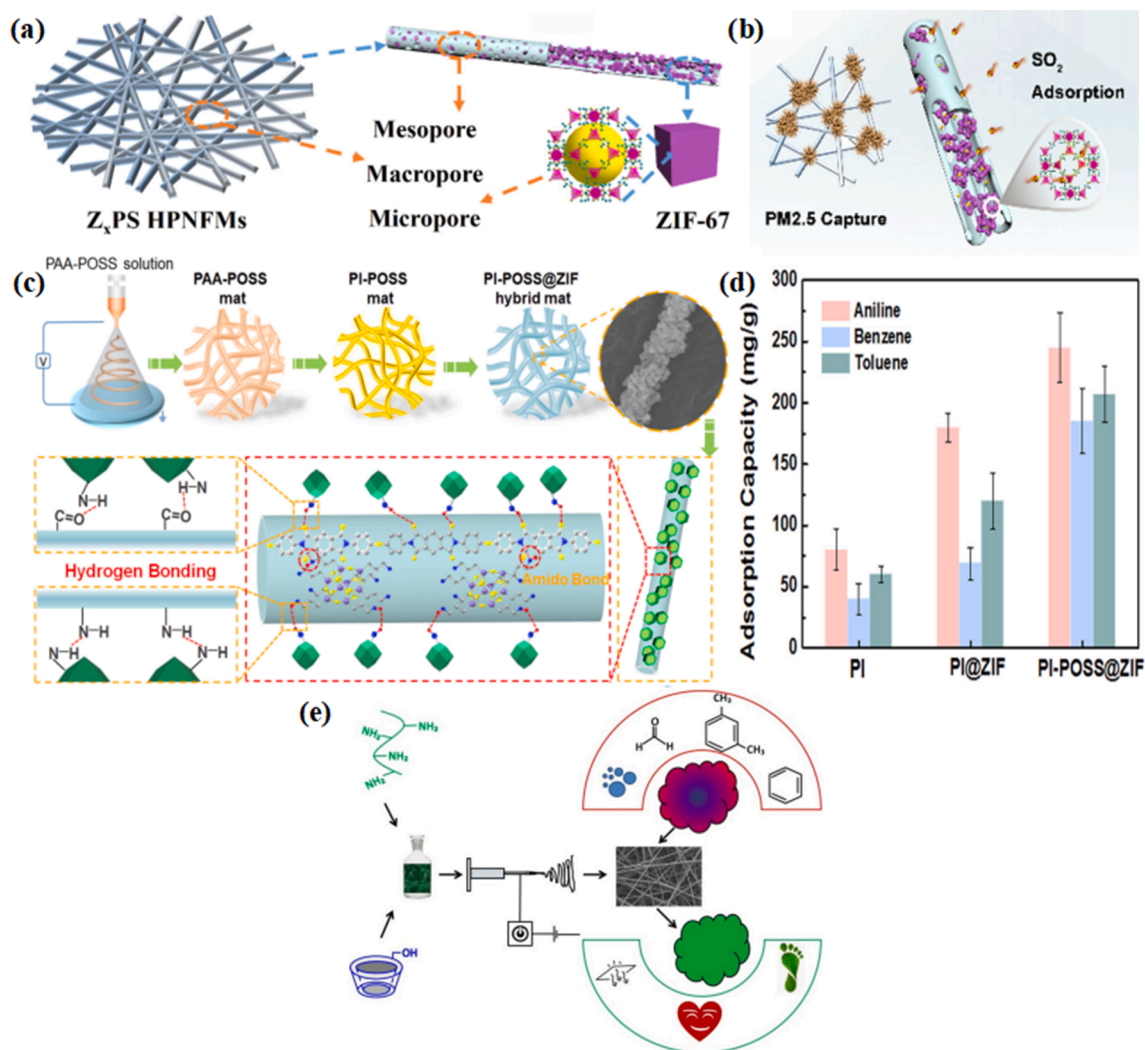
Fig. 15. (a) Structure of PS/ZIF–67 porous nanofibers. (b) Filtration and SO$_2$ adsorption process of PS/ZIF–67 fibers [183]. (c) Fabrication process of PI–POSS@ZIF membrane. (d) Adsorption capacity of different membranes [158]. (e) Schematic illustration for the fabrication process of gelatin/β–cyclodextrin nanofibers [182].

(242 mg/g) and formaldehyde (0.75 mg/g). The filtration efficiency for 0.3 μm particles was 97 %, the pressure drop was 148 Pa and the QF was 0.029 Pa^{-1} [182]. Obviously, the air filtration performance of these kinds of all–polymer nanofibrous membranes still needs to be further improved.

4.5. High–performance electrospun air filter with multiple functions

Endowing high efficiency electrospun air filter with multiple functions is the research focus in the future. On the premise of meeting the performance of high efficiency and low resistance air filtration, the realization of more performances and good coupling are expected. The existing research on electrospun multifunctional air filters are shown in Table 1. Apparently, few studies have successfully coupled multiple functions (greater than two functions). Among them, the antibacterial performance and gaseous pollutants absorption often depend on the introduced functional material itself, while the dust holding capacity and water vapor transport depend more on the structure of the air filter. Therefore, in the case of meeting the first two functions at the same time, the load of realizing the latter two functions will be more expected to realize the integration of all functions, which still needs further exploration.

5. Conclusions and perspectives

With the increasingly serious air pollution and the constant threat of viruses transmitted from aerosols, the demand for air filter used for personal protection is becoming more and more urgent. Electrospun air filter can achieve high efficiency and low resistance air filtration because of its small diameter, highly interconnected through holes and adjustable structure. However, it is inappropriate to blindly pursuing the excessive improvement of filtration performance: giving more functions to the air filter will greatly increase the profits for personal protection, which can be realized more easily and simply through electrospinning. This review focuses on the mechanism of high efficiency and low resistance air filtration from the perspective of membrane; electrospun preparation method and its characteristic; the realization of various functions for maximizing personal protection benefits, in the hope of providing guidance for the preparation of high–performance air filter with multiple functions to realize better personal protection.

Although much progress has been made in multifunctional electrospun air filter for personal protection, there are still many challenges: (I) The mechanical properties of existing electrospun filter are often insufficient, which will affect its filtration performance, long–term use and reuse capacity, and bring a burden to the environment. (II) The preparation of electrospun filter using degradable materials and green solvents will also reduce the burden of the environment, but these

Table 1

Existing high–performance electrospun air filters with multiple functions.

functions	materials	filtration mechanism	PMs (μm)	air velocity (default to cm/s)	efficiency (%)	resistance (default to Pa)	QF (Pa–1)	ref
high dust holding capacity only	PSU/PAN/PA–6	enhanced electrostatic adsorption & improved slip effect	0.3	5.3	99.992	118	0.080	[67]
	TPU/PS/PA–6	enhanced electrostatic adsorption & improved slip effect	0.3	5.3	99.99	54	0.170	[68]
	PAN	enhanced electrostatic adsorption & improved slip effect	0.3	5.3	99.99	92	0.100	[143]
	PA–6/PMIA	improved slip effect	0.3–0.5	5.3	99.995	101	0.098	[41]
	PA–56	improved slip effect	0.3–0.5	5.3	99.995	111	0.089	[185]
water vapor transfer only	PAN/PEI	enhanced electrostatic adsorption & improved slip effect & increased contact sites	0.3	5.3	99.3	64	0.109	[172]
	PVDF/PAN@SiO$_2$	enhanced electrostatic adsorption & improved slip effect & increased contact sites	0.3	not mentioned	99.96	86	0.091	[170]
antibacterial activity only	TiO$_2$/CS/PVA	enhanced electrostatic adsorption & increased contact sites	2.5	80	95.2	127.5	0.024	[175]
	PAN/PVP/CNT	enhanced electrostatic adsorption & improved slip effect	0.3	5.3	99.994	49	0.198	[186]
	PCL/zein/Ag	enhanced electrostatic adsorption & improved slip effect & increased contact sites	0.3	20 L/min	97.19	350	0.010	[187]
	PVA/PEO/CNF/TiO$_2$	enhanced electrostatic adsorption & improved slip effect & increased contact sites	0.075	not mentioned	98.7	83.4 L/min	not mentioned	[173]
	PVA/CS/N–halamine	enhanced electrostatic adsorption & improved slip effect	0.3	32 L/min	99.3	183	0.027	[176]
	PVDF/Ag	enhanced electrostatic adsorption & improved slip effect & increased contact sites	0.3	85 L/min	99.95	137.5	0.055	[180]
	ZnO@PVA/KGM	enhanced electrostatic adsorption & improved slip effect & increased contact sites	0.3	32 L/min	99.99	130	0.071	[159]
	PVA/PAA/SiO$_2$/Ag	enhanced electrostatic adsorption & increased contact sites	0.3	32 L/min	98.85	132	0.034	[174]
	PA6/PVP@CS@Cur	enhanced electrostatic adsorption & improved slip effect	0.3	5.3	99.83	54	0.118	[153]
	PLA/PCL/Ag/Zn	enhanced electrostatic adsorption & improved slip effect & increased contact sites	0.3	33 L/min	99.93	100	0.073	[6]
	PVDF/ZIF–8	enhanced electrostatic adsorption & improved slip effect & increased contact sites	0.3	35 L/min	99.9	71	0.097	[32]
	PVDF/PS/Zn/Ag	enhanced electrostatic adsorption & improved slip effect & increased contact sites	0.3	85 L/min	99.1	79.2	0.059	[31]
gaseous pollutants absorption only	PAN/β–CD	enhanced electrostatic adsorption	0.3	32 L/min	95	112	0.026	[184]
	PI–POSS@ZIF–8	enhanced electrostatic adsorption & increased contact sites	0.3	5.3	99.28	49.21	0.100	[158]
	ZIF–67/PS	enhanced electrostatic adsorption & increased contact sites	0.3	5.3	99.921	91	0.078	[183]
	Gelatin/β–CD	enhanced electrostatic adsorption	0.3	6	97	148	0.029	[182]
water vapor transfer & gaseous pollutants absorption	PAN/β–CD/PCL/ZnO	enhanced electrostatic adsorption & improved slip effect & increased contact sites	0.01–10	not mentioned	99.99	156.5	0.059	[164]
	PS/PAN@ZIF–8	enhanced electrostatic adsorption & improved slip effect & increased contact sites	0.3	5.3	99.973	80.1	0.103	[171]
antibacterial activity & gaseous pollutants absorption	PET/PE/PVP@ZIF–8	enhanced electrostatic adsorption & increased contact sites	0.3	5.3	90.26	62.74	0.037	[125]

materials often have insufficient electrospun properties, and the filtration performance of the prepared filter is difficult to guarantee. (III) The exploration and in–depth study of more performances based on existing research will further increase the protection benefits, such as ultraviolet absorption, thermal radiation, etc. (IV) The realization of multifunctional often requires more preparation processes, thus, exploring the optimized electrospinning strategy to realize the most simplified preparation (i.e., one–step preparation) will better support the batch preparation and industrial production of multifunctional electrospun air filter. (V) Effectively predicting the service life of high–performance air filter (including the service life of filter performance and other functions) will avoid the danger caused by the attenuation of protection performance, or the discomfort caused by the attenuation of other functional capabilities [188]. Therefore, the development of new computing methods for future materials and equipment based on artificial intelligence (AI) will solve this problem. At present, there are performance predictions for lithium batteries and supercapacitors based on AI calculation methods, but there is less research on performance prediction for air filter [189–192].

CRediT authorship contribution statement

Zungui Shao: Methodology, Formal analysis, Investigation, Writing – original draft. **Huatan Chen:** Formal analysis, Writing – review & editing. **Qingfeng Wang:** Formal analysis, Validation, Writing – review & editing. **Guoyi Kang:** Formal analysis, Writing – review & editing. **Xiang Wang:** Funding acquisition, Resources. **Wenwang Li:** Funding acquisition, Resources. **Yifang Liu:** Funding acquisition, Resources. **Gaofeng Zheng:** Methodology, Formal analysis, Funding acquisition, Supervision, Resources.

Declaration of Competing Interest

The authors declare that they have no known competing financial interests or personal relationships that could have appeared to influence the work reported in this paper.

Data availability

No data was used for the research described in the article.

Acknowledgments

References

[1] J. Li, S. Lai, G.F. Gao, W. Shi, The emergence, genomic diversity and global spread of SARS-CoV-2, Nature 600 (2021) 408–418.

[2] J.S. Turner, W. Kim, E. Kalaidina, C.W. Goss, A.M. Rauseo, A.J. Schmitz, L. Hansen, A. Haile, M.K. Klebert, I. Pusic, J.A. O'Halloran, R.M. Presti, A. H. Ellebedy, SARS-CoV-2 infection induces long-lived bone marrow plasma cells in humans, Nature 595 (2021) 421–425.

[3] D. Planas, D. Veyer, A. Baidaliuk, I. Staropoli, F. Guivel-Benhassine, M.M. Rajah, C. Planchais, F. Porrot, N. Robillard, J. Puech, M. Prot, F. Gallais, P. Gantner, A. Velay, J. Le Guen, N. Kassis-Chikhani, D. Edriss, L. Belec, A. Seve, L. Courtellemont, H. Pere, L. Hocqueloux, S. Fafi-Kremer, T. Prazuck, H. Mouquet, T. Bruel, E. Simon-Loriere, F.A. Rey, O. Schwartz, Reduced sensitivity of SARS-CoV-2 variant Delta to antibody neutralization, Nature 596 (2021) 276–280.

[4] W. Deng, Y. Sun, X. Yao, K. Subramanian, C. Ling, H. Wang, S.S. Chopra, B.B. Xu, J.X. Wang, J.F. Chen, D. Wang, H. Amancio, S. Pramana, R. Ye, S. Wang, Masks for COVID-19, Adv. Sci. 9 (2022) e2102189.

[5] C. Lyu, P. Zhao, J. Xie, S. Dong, J. Liu, C. Rao, J. Fu, Electrospinning of nanofibrous membrane and its applications in air filtration: A review, Nanomaterials 11 (2021) 1501.

[6] Y. Cheng, J. Li, M. Chen, S. Zhang, R. He, N. Wang, Environmentally friendly and antimicrobial bilayer structured fabrics with integrated interception and sterilization for personal protective mask, Sep. Purif. Technol. 294 (2022), 121165.

[7] D. Yang, Y. Zhu, J. Li, Z. Yue, J. Zhou, X. Wang, Degradable, antibacterial and ultrathin filtrating electrospinning membranes of Ag-MOFs/poly(l-lactide) for air pollution control and medical protection, Int. J. Biol. Macromol. 212 (2022) 182–192.

[8] A. Mamun, T. Blachowicz, L. Sabantina, Electrospun nanofiber mats for filtering applications-technology, structure and materials, Polymers 13 (2021) 1368.

[9] W.K. Essa, S.A. Yasin, I.A. Saeed, G.A.M. Ali, Nanofiber-based face masks and respirators as COVID-19 protection: A review, Membranes 11 (2021) 250.

[10] J. Xu, X. Xiao, W. Zhang, R. Xu, S.C. Kim, Y. Cui, T.T. Howard, E. Wu, Y. Cui, Air-Filtering Masks for Respiratory Protection from PM2.5 and Pandemic Pathogens, One, Earth 3 (2020) 574–589.

[11] D. Lv, M. Zhu, Z. Jiang, S. Jiang, Q. Zhang, R. Xiong, C. Huang, Green Electrospun Nanofibers and Their Application in Air Filtration, Macromol. Mater. Eng. 303 (2018) 1800336.

[12] D.Y. Choi, S.H. Jung, D.K. Song, E.J. An, D. Park, T.O. Kim, J.H. Jung, H.M. Lee, Al-Coated Conductive Fibrous Filter with Low Pressure Drop for Efficient Electrostatic Capture of Ultrafine Particulate Pollutants, ACS Appl. Mater. Interfaces 9 (2017) 16495–16504.

[13] M. Zhu, J. Han, F. Wang, W. Shao, R. Xiong, Q. Zhang, H. Pan, Y. Yang, S. K. Samal, F. Zhang, C. Huang, Electrospun Nanofibers Membranes for Effective Air Filtration, Macromol. Mater. Eng. 302 (2017) 1600353.

[14] T. Lu, J. Cui, Q. Qu, Y. Wang, J. Zhang, R. Xiong, W. Ma, C. Huang, Multistructured Electrospun Nanofibers for Air Filtration: A Review, ACS Appl. Mater. Interfaces 13 (2021) 23293–23313.

[15] K. O'Dowd, K.M. Nair, P. Forouzandeh, S. Mathew, J. Grant, R. Moran, J. Bartlett, J. Bird, S.C. Pillai, Face Masks and Respirators in the Fight against the COVID-19 Pandemic: A Review of Current Materials, Advances and Future Perspectives, Materials 13 (2020) 3363.

[16] E. Hossain, S. Bhadra, H. Jain, S. Das, A. Bhattacharya, S. Ghosh, D. Levine, Recharging and rejuvenation of decontaminated N95 masks, Phys. Fluids 32 (2020), 093304.

[17] D. Chen, L. Tang, Y. Wang, Y. Tan, Y. Fu, W. Cai, Z. Yu, S. Sun, J. Zheng, J. Cui, G. Wang, Y. Liu, H. Zhou, Speaking-Induced Charge-Laden Face Masks with Durable Protectiveness and Wearing Breathability, ACS Appl. Mater. Interfaces 14 (2022) 17774–17782.

[18] J. Cui, T. Lu, F. Li, Y. Wang, J. Lei, W. Ma, Y. Zou, C. Huang, Flexible and transparent composite nanofibre membrane that was fabricated via a "green" electrospinning method for efficient particulate matter 2.5 capture, J. Colloid Interface Sci. 582 (2021) 506–514.

[19] L.M. Valencia-Osorio, M.L. Álvarez-Láinez, Global View and Trends in Electrospun Nanofiber Membranes for Particulate Matter Filtration: A Review, Macromol. Mater. Eng. 306 (2021) 2100278.

[20] R. Xiong, D. Hua, J. Van Hoeck, D. Berdecka, L. Leger, S. De Munter, J.C. Fraire, L. Raes, A. Harizaj, F. Sauvage, G. Goetgeluk, M. Pille, J. Aalders, J. Belza, T. Van Acker, E. Bolea-Fernandez, T. Si, F. Vanhaecke, W.H. De Vos, B. Vandekerckhove, J. van Hengel, K. Raemdonck, C. Huang, S.C. De Smedt, K. Braeckmans, Photothermal nanofibres enable safe engineering of therapeutic cells, Nat. Nanotechnol. 16 (2021) 1281–1291.

[21] J. Jjagwe, P.W. Olupot, E. Menya, H.M. Kalibbala, Synthesis and Application of Granular Activated Carbon from Biomass Waste Materials for Water Treatment: A Review, J. Bioresour. Bioproducts 6 (2021) 292–322.

[22] S. Ramakrishna, K. Fujihara, W.-E. Teo, T. Yong, Z. Ma, R. Ramaseshan, Electrospun nanofibers: solving global issues, Mater. Today 9 (2006) 40–50.

[23] V. Thavasi, G. Singh, S. Ramakrishna, Electrospun nanofibers in energy and environmental applications, Energy Environ. Sci. 1 (2008) 205–221.

[24] J. Xue, X. Xie, W. Liu, Y.X. Xia, Electrospun Nanofibers: New Concepts, Materials, and Applications, Acc. Chem. Res. 50 (2017) 1976–1987.

[25] Z. Yang, X. Zhang, Z. Qin, H. Li, J. Wang, G. Zeng, C. Liu, J. Long, Y. Zhao, Y. Li, G. Yan, Airflow Synergistic Needleless Electrospinning of Instant Noodle-like Curly Nanofibrous Membranes for High-Efficiency Air Filtration, Small 18 (2022) e2107250.

[26] J. Hu, Z. Xiong, Y. Liu, J. Lin, A biodegradable composite filter made from electrospun zein fibers underlaid on the cellulose paper towel, Int. J. Biol. Macromol. 204 (2022) 419–428.

[27] C. Zhou, W. Han, X. Yang, H. Fan, C. Li, L. Dong, H. Meng, Electrospun polyetherimide/zeolitic imidazole framework nanofibrous membranes for enhanced air filtration performance under high temperature and high humidity conditions, Chem. Eng. J. 433 (2022), 134069.

[28] T. Dong, Y. Hua, X. Zhu, X. Huang, S. Chi, Y. Liu, C.-W. Lou, J.-H. Lin, Highly Efficient and Sustainable PM Filtration Using Piezo Nanofibrous Membrane with Gradient Shrinking Porous Network, Sep. Purif. Technol. 289 (2022) 120753.

[29] J. Liu, C. Ding, F.O. Dunne, Y. Guo, X. Fu, W.H. Zhong, A Bimodal Protein Fabric Enabled via In Situ Diffusion for High-Performance Air Filtration, Environ. Sci. Technol. 54 (2020) 10242–10250.

[30] Y. Deng, T. Lu, J. Cui, S. Keshari Samal, R. Xiong, C. Huang, Bio-based electrospun nanofiber as building blocks for a novel eco-friendly air filtration membrane: A review, Sep. Purif. Technol. 277 (2021), 119623.

[31] R. He, J. Li, M. Chen, S. Zhang, Y. Cheng, X. Ning, N. Wang, Tailoring moisture electroactive Ag/Zn@cotton coupled with electrospun PVDF/PS nanofibers for antimicrobial face masks, J. Hazard. Mater. 428 (2022), 128239.

[32] Q. Geng, S. Dong, Y. Li, H. Wu, X. Yang, X. Ning, D. Yuan, High-Performance photoinduced antimicrobial membrane toward efficient PM2.5-0.3 capture and Oil-Water separation, Sep. Purif. Technol. 284 (2022), 120267.

[33] T. Lu, Y. Deng, J. Cui, W. Cao, Q. Qu, Y. Wang, R. Xiong, W. Ma, J. Lei, C. Huang, Multifunctional Applications of Blow-Spinning Setaria viridis Structured Fibrous Membranes in Water Purification, ACS Appl. Mater. Interfaces 13 (2021) 22874–22883.

[34] J. Yang, Y. Zhang, L. Zhou, F. Zhang, Y. Jing, M. Huang, H. Liu, Quality-related monitoring of papermaking wastewater treatment processes using dynamic multiblock partial least squares, J. Bioresour. Bioproducts 7 (2022) 73–82.

[35] M. Zhu, R. Xiong, C. Huang, Bio-based and photocrosslinked electrospun antibacterial nanofibrous membranes for air filtration, Carbohydr. Polym. 205 (2019) 55–62.

[36] K. Huang, W. Sun, G. Feng, J. Wang, J. Song, Indoor air quality analysis of 8 mechanically ventilated residential buildings in northeast China based on long-term monitoring, Sustain. Cities Soc. 54 (2020), 101947.

[37] Y. Zhou, Y. Liu, M. Zhang, Z. Feng, D.G. Yu, K. Wang, Electrospun Nanofiber Membranes for Air Filtration: A Review, Nanomaterials 12 (2022) 1077.

[38] B. Robert, G. Nallathambi, A concise review on electrospun nanofibres/nanonets for filtration of gaseous and solid constituents (PM2.5) from polluted air, Colloids Interface, Sci. Commun. 37 (2020), 100275.

[39] Y. Li, X. Yin, J. Yu, B. Ding, Electrospun nanofibers for high-performance air filtration, Compos. Commun. 15 (2019) 6–19.

[40] M. Chen, J. Jiang, S. Feng, Z.-X. Low, Z. Zhong, W. Xing, Graphene oxide functionalized polyvinylidene fluoride nanofibrous membranes for efficient particulate matter removal, J. Membr. Sci. 635 (2021), 119463.

[41] S. Zhang, H. Liu, J. Yu, W. Luo, B. Ding, Microwave structured polyamide-6 nanofiber/net membrane with embedded poly(m-phenylene isophthalamide) staple fibers for effective ultrafine particle filtration, J. Mater. Chem. A 4 (2016) 6149–6157.

[42] X. Chen, Y. Xu, M. Liang, Q. Ke, Y. Fang, H. Xu, X. Jin, C. Huang, Honeycomb-like polysulphone/polyurethane nanofiber filter for the removal of organic/inorganic species from air streams, J. Hazard. Mater. 347 (2018) 325–333.

[43] Q. Geng, Y. Pu, Y. Li, X. Yang, H. Wu, S. Dong, D. Yuan, X. Ning, Multi-Component Nanofiber Composite Membrane Enabled High PM0.3 Removal Efficiency and Oil/Water Separation Performance in Complex Environment, J. Hazard. Mater. 422 (2022), 126835.

[44] S. Jung, J. Kim, Advanced Design of Fiber-Based Particulate Filters: Materials, Morphology, and Construction of Fibrous Assembly, Polymers 12 (2020) 1714.

[45] D.N. Phan, M.Q. Khan, N.T. Nguyen, T.T. Phan, A. Ullah, M. Khatri, N.N. Kien, I. S. Kim, A review on the fabrication of several carbohydrate polymers into nanofibrous structures using electrospinning for removal of metal ions and dyes, Carbohydr. Polym. 252 (2021), 117175.

[46] F. Cui, W. Han, J. Ge, X. Wu, H. Kim, B. Ding, Electrospinning: A versatile strategy for mimicking natural creatures, Compos. Commun. 10 (2018) 175–185.

[47] A. Barhoum, K. Pal, H. Rahier, H. Uludag, I.S. Kim, M. Bechelany, Nanofibers as new-generation materials: From spinning and nano-spinning fabrication techniques to emerging applications, Appl. Mater. Today 17 (2019) 1–35.

[48] H. Saleem, L. Trabzon, A. Kilic, S.J. Zaidi, Recent advances in nanofibrous membranes: Production and applications in water treatment and desalination, Desalination 478 (2020), 114178.

[49] E.I. El-Aswar, H. Ramadan, H. Elkik, A.G. Taha, A comprehensive review on preparation, functionalization and recent applications of nanofiber membranes in wastewater treatment, J. Environ. Manage. 301 (2022), 113908.

[50] J. Tang, Y. Wu, S. Ma, T. Yan, Z. Pan, Flexible strain sensor based on CNT/TPU composite nanofiber yarn for smart sports bandage, Compos. B. Eng. 232 (2022), 109605.

[51] S. Shi, Y. Si, Y. Han, T. Wu, M.I. Iqbal, B. Fei, R.K.Y. Li, J. Hu, J. Qu, Recent Progress in Protective Membranes Fabricated via Electrospinning: Advanced Materials, Biomimetic Structures, and Functional Applications, Adv. Mater. 34 (2022) e2107938.

[52] F. Zhou, C. Cui, S. Sun, S. Wu, S. Chen, J. Ma, C.M. Li, Electrospun ZnO-loaded chitosan/PCL bilayer membranes with spatially designed structure for accelerated wound healing, Carbohydr. Polym. 282 (2022), 119131.

[53] R. Barhate, S. Ramakrishna, Nanofibrous filtering media: Filtration problems and solutions from tiny materials, J. Membr. Sci. 296 (2007) 1–8.

[54] A. Konda, A. Prakash, G.A. Moss, M. Schmoldt, G.D. Grant, S. Guha, Aerosol Filtration Efficiency of Common Fabrics Used in Respiratory Cloth Masks, ACS Nano 14 (2020) 6339–6347.

[55] X. Wang, B. Ding, G. Sun, M. Wang, J. Yu, Electro-spinning/netting: A strategy for the fabrication of three-dimensional polymer nano-fiber/nets, Prog. Mater. Sci. 58 (2013) 1173–1243.

[56] R. Thakur, D. Das, A. Das, Electret Air Filters, Sep. Purif. Rev. 42 (2013) 87–129.

[57] Y. Gao, E. Tian, Y. Zhang, J. Mo, Utilizing electrostatic effect in fibrous filters for efficient airborne particles removal: Principles, fabrication, and material properties, Appl. Mater. Today 26 (2022), 101369.

[58] T. Xia, Y. Bian, L. Zhang, C. Chen, Relationship between pressure drop and face velocity for electrospun nanofiber filters, Energy Build. 158 (2018) 987–999.

[59] W. Sambaer, M. Zatloukal, D. Kimmer, 3D modeling of filtration process via polyurethane nanofiber based nonwoven filters prepared by electrospinning process, Chem. Eng. Sci. 66 (2011) 613–623.

[60] Z. Quan, Y. Zu, Y. Wang, M. Zhou, X. Qin, J. Yu, Slip effect based bimodal nanofibrous membrane for high-efficiency and low-resistance air purification, Sep. Purif. Technol. 275 (2021), 119258.

[61] P. Li, C. Wang, Y. Zhang, F. Wei, Air filtration in the free molecular flow regime: a review of high-efficiency particulate air filters based on carbon nanotubes, Small 10 (2014) 4543–4561.

[62] Z. Zhang, B.Y.H. Liu, Experimental Study of Aerosol Filtration in the Transition Flow Regime, Aerosol Sci. Tech. 16 (1992) 227–235.

[63] L. Bao, K. Seki, H. Niinuma, Y. Otani, R. Balgis, T. Ogi, K. Okuyama, Verification of slip flow in nanofiber filter media through pressure drop measurement at low-pressure conditions, Sep. Purif. Technol. 159 (2016) 100–107.

[64] J. Matulevicius, L. Kliucininkas, D. Martuzevicius, E. Krugly, M. Tichonovas, J. Baltrusaitis, Design and Characterization of Electrospun Polyamide Nanofiber Media for Air Filtration Applications, J. Nanomater. 2014 (2014) 1–13.

[65] F. Zuo, S. Zhang, H. Liu, H. Fong, X. Yin, J. Yu, B. Ding, Free-Standing Polyurethane Nanofiber/Nets Air Filters for Effective PM Capture, Small 13 (2017) 1702139.

[66] H. Dai, X. Liu, C. Zhang, K. Ma, Y. Zhang, Electrospinning Polyacrylonitrile/Graphene Oxide/Polyimide nanofibrous membranes for High-efficiency PM2.5 filtration, Sep. Purif. Technol. 276 (2021), 119243.

[67] S. Zhang, N. Tang, L. Cao, X. Yin, J. Yu, B. Ding, Highly Integrated Polysulfone/Polyacrylonitrile/Polyamide-6 Air Filter for Multilevel Physical Sieving Airborne Particles, ACS Appl. Mater. Interfaces 8 (2016) 29062–29072.

[68] J.-P. Chen, S.-C. Chen, X.-Q. Wu, X.-X. Ke, R.-X. Wu, Y.-M. Zheng, Multilevel structured TPU/PS/PA-6 composite membrane for high-efficiency airborne particles capture: Preparation, performance evaluation and mechanism insights, J. Membr. Sci. 633 (2021) 119392.

[69] R. Balgis, H. Murata, Y. Goi, T. Ogi, K. Okuyama, L. Bao, Synthesis of Dual-Size Cellulose-Polyvinylpyrrolidone Nanofiber Composites via One-Step Electrospinning Method for High-Performance Air Filter, Langmuir 33 (2017) 6127–6134.

[70] J. Xiong, W. Shao, L. Wang, C. Cui, Y. Gao, Y. Jin, H. Yu, P. Han, F. Liu, J. He, High-performance anti-haze window screen based on multiscale structured polyvinylidene fluoride nanofibers, J. Colloid Interface Sci. 607 (2022) 711–719.

[71] W.-W.-F. Leung, C.-H. Hung, P.-T. Yuen, Effect of face velocity, nanofiber packing density and thickness on filtration performance of filters with nanofibers coated on a substrate, Sep. Purif. Technol. 71 (2010) 30–37.

[72] F. Deuber, S. Mousavi, L. Federer, M. Hofer, C. Adlhart, Exploration of Ultralight Nanofiber Aerogels as Particle Filters: Capacity and Efficiency, ACS Appl. Mater. Interfaces 10 (2018) 9069–9076.

[73] Z. Zhu, Y. Zhang, L. Bao, J. Chen, S. Duan, S.-C. Chen, P. Xu, W.-N. Wang, Self-decontaminating nanofibrous filters for efficient particulate matter removal and airborne bacteria inactivation, Environ. Sci. Nano 8 (2021) 1081–1095.

[74] R. Al-Attabi, Y. Morsi, W. Kujawski, L. Kong, J.A. Schütz, L.F. Dumée, Wrinkled silica doped electrospun nano-fiber membranes with engineered roughness for advanced aerosol air filtration, Sep. Purif. Technol. 215 (2019) 500–507.

[75] X. Huang, T. Jiao, Q. Liu, L. Zhang, J. Zhou, B. Li, Q. Peng, Hierarchical electrospun nanofibers treated by solvent vapor annealing as air filtration mat for high-efficiency PM2.5 capture, Sci. China Mater. 62 (2018) 423–436.

[76] L. Jing, K. Shim, C.Y. Toe, T. Fang, C. Zhao, R. Amal, K.N. Sun, J.H. Kim, Y.H. Ng, Electrospun Polyacrylonitrile-Ionic Liquid Nanofibers for Superior PM2.5 Capture Capacity, ACS Appl. Mater. Interfaces 8 (2016) 7030–7036.

[77] Y. Deng, T. Lu, X. Zhang, Z. Zeng, R. Tao, Q. Qu, Y. Zhang, M. Zhu, R. Xiong, C. Huang, Multi-hierarchical nanofiber membrane with typical curved-ribbon structure fabricated by green electrospinning for efficient, breathable and sustainable air filtration, J. Membr. Sci. 660 (2022).

[78] C.H. Jung, K.W. Lee, Analytic Solution for Diffusional Filtration across Granular Beds in Low Knudsen Number Regime, Part. Part. Syst. Charact. 21 (2004) 234–242.

[79] S. Wang, X. Zhao, X. Yin, J. Yu, B. Ding, Electret Polyvinylidene Fluoride Nanofibers Hybridized by Polytetrafluoroethylene Nanoparticles for High-Efficiency Air Filtration, ACS Appl. Mater. Interfaces 8 (2016) 23985–23994.

[80] Y. Wang, Y. Xu, D. Wang, Y. Zhang, X. Zhang, J. Liu, Y. Zhao, C. Huang, X. Jin, Polytetrafluoroethylene/Polyphenylene Sulfide Needle-Punched Triboelectric Air Filter for Efficient Particulate Matter Removal, ACS Appl. Mater. Interfaces 11 (2019) 48437–48449.

[81] P. Zhang, S. Zhang, D. Wan, P. Zhang, Z. Zhang, G. Shao, Multilevel polarization-fields enhanced capture and photocatalytic conversion of particulate matter over flexible schottky-junction nanofiber membranes, J. Hazard. Mater. 395 (2020), 122639.

[82] H. Gao, W. He, Y.-B. Zhao, D.M. Opris, G. Xu, J. Wang, Electret mechanisms and kinetics of electrospun nanofiber membranes and lifetime in filtration applications in comparison with corona-charged membranes, J. Membr. Sci. 600 (2020), 117879.

[83] X. Li, N. Wang, G. Fan, J. Yu, J. Gao, G. Sun, B. Ding, Electreted polyetherimide-silica fibrous membranes for enhanced filtration of fine particles, J. Colloid Interface Sci. 439 (2015) 12–20.

[84] H. Wan, N. Wang, J. Yang, Y. Si, K. Chen, B. Ding, G. Sun, M. El-Newehy, S.S. Al-Deyab, J. Yu, Hierarchically structured polysulfone/titania fibrous membranes with enhanced air filtration performance, J. Colloid Interface Sci. 417 (2014) 18–26.

[85] N. Wang, M. Cai, X. Yang, Y. Yang, Electret nanofibrous membrane with enhanced filtration performance and wearing comfortability for face mask, J. Colloid Interface Sci. 530 (2018) 695–703.

[86] P. Jiang, X. Zhao, Y. Li, Y. Liao, T. Hua, X. Yin, J. Yu, B. Ding, Moisture and oily molecules stable nanofibrous electret membranes for effectively capturing PM 2.5, Compos. Commun. 6 (2017) 34–40.

[87] B. Wang, Z. Sun, Q. Sun, J. Wang, Z. Du, C. Li, X. Li, The preparation of bifunctional electrospun air filtration membranes by introducing attapulgite for the efficient capturing of ultrafine PMs and hazardous heavy metal ions, Environ. Pollut. 249 (2019) 851–859.

[88] X. Yang, Y. Pu, S. Li, X. Liu, Z. Wang, D. Yuan, X. Ning, Electrospun Polymer Composite Membrane with Superior Thermal Stability and Excellent Chemical Resistance for High-Efficiency PM2.5 Capture, ACS Appl. Mater. Interfaces 11 (2019) 43188–43199.

[89] Y. Li, L. Cao, X. Yin, Y. Si, J. Yu, B. Ding, Ultrafine, self-crimp, and electret nano-wool for low-resistance and high-efficiency protective filter media against PM0.3, J. Colloid Interface Sci. 578 (2020) 565–573.

[90] A. Wang, X. Li, T. Hou, Y. Lu, J. Zhou, X. Zhang, B. Yang, High efficiency, low resistance and high temperature resistance PTFE porous fibrous membrane for air filtration, Mater. Lett. 295 (2021), 129831.

[91] R.R. Cai, S.Z. Li, L.Z. Zhang, Y. Lei, Fabrication and performance of a stable micro/nano composite electret filter for effective PM2.5 capture, Sci. Total Environ. 725 (2020), 138297.

[92] L. Quoc Pham, M.V. Uspenskaya, R.O. Olekhnovich, R.A. Olvera Bernal, A Review on Electrospun PVC Nanofibers: Fabrication, Properties, and Application, Fibers 9 (2021) 12.

[93] Y. Li, X. Yin, Y. Si, J. Yu, B. Ding, All-polymer hybrid electret fibers for high-efficiency and low-resistance filter media, Chem. Eng. J. 398 (2020), 125626.

[94] C. Pang, H. Wang, X. Lin, Ultralight ethyl cellulose-based electret fiber membrane for low-resistance and high-efficient capture of PM2.5, Colloids Surf. A Physicochem. Eng. Asp. 630 (2021), 127643.

[95] S. Wu, R. Cai, L. Zhang, Research progress on the cleaning and regeneration of PM2.5 filter media, Particuology 57 (2021) 28–44.

[96] B.M. Cho, Y.S. Nam, J.Y. Cheon, W.H. Park, Residual charge and filtration efficiency of polycarbonate fibrous membranes prepared by electrospinning, J. Appl. Polym. Sci. 132 (2015) 41340.

[97] H.J. Kim, S.J. Park, D.I. Kim, S. Lee, O.S. Kwon, I.K. Kim, Moisture Effect on Particulate Matter Filtration Performance using Electro-Spun Nanofibers including Density Functional Theory Analysis, Sci. Rep. 9 (2019) 7015.

[98] S. Chen, C. Gao, W. Tang, H. Zhu, Y. Han, Q. Jiang, T. Li, X. Cao, Z. Wang, Self-powered cleaning of air pollution by wind driven triboelectric nanogenerator, Nano Energy 14 (2015) 217–225.

[99] S. Ding, Y. Cao, F. Huang, Y. Wang, J. Li, S. Chen, Spontaneous polarization induced electrostatic charge in washable electret composite fabrics for reusable air-filtering application, Compos. Sci. Technol. 217 (2022), 109093.

[100] Y. Liu, M. Park, B. Ding, J. Kim, M. El-Newehy, S.S. Al-Deyab, H.-Y. Kim, Facile electrospun Polyacrylonitrile/poly(acrylic acid) nanofibrous membranes for high efficiency particulate air filtration, Fibers Polym. 16 (2015) 629–633.

[101] Y. Hu, Y. Wang, S. Tian, A. Yu, L. Wan, J. Zhai, Performance-Enhanced and Washable Triboelectric Air Filter Based on Polyvinylidene Fluoride/UiO-66 Composite Nanofiber Membrane, Macromol. Mater. Eng. 306 (2021) 2100128.

[102] S. Lee, A.R. Cho, D. Park, J.K. Kim, K.S. Han, I.J. Yoon, M.H. Lee, J. Nah, Reusable Polybenzimidazole Nanofiber Membrane Filter for Highly Breathable PM2.5 Dust Proof Mask, ACS Appl. Mater. Interfaces 11 (2019) 2750–2757.

[103] G.H. Zhang, Q.H. Zhu, L. Zhang, F. Yong, Z. Zhang, S.L. Wang, Y. Wang, L. He, G. H. Tao, High-performance particulate matter including nanoscale particle removal by a self-powered air filter, Nat. Commun. 11 (2020) 1653.

[104] Z.L. Wang, A.C. Wang, On the origin of contact-electrification, Mater. Today 30 (2019) 34–51.

[105] G.Q. Gu, C.B. Han, C.X. Lu, C. He, T. Jiang, Z.L. Gao, C.J. Li, Z.L. Wang, Triboelectric Nanogenerator Enhanced Nanofiber Air Filters for Efficient Particulate Matter Removal, ACS Nano 11 (2017) 6211–6217.

[106] G. Liu, J. Nie, C. Han, T. Jiang, Z. Yang, Y. Pang, L. Xu, T. Guo, T. Bu, C. Zhang, Z. L. Wang, Self-Powered Electrostatic Adsorption Face Mask Based on a Triboelectric Nanogenerator, ACS Appl. Mater. Interfaces 10 (2018) 7126–7133.

[107] Z. Shao, J. Jiang, X. Wang, W. Li, L. Fang, G. Zheng, Self-Powered Electrospun Composite Nanofiber Membrane for Highly Efficient Air Filtration, Nanomaterials 10 (2020) 1706.

[108] Y. Bai, C.B. Han, C. He, G.Q. Gu, J.H. Nie, J.J. Shao, T.X. Xiao, C.R. Deng, Z. L. Wang, Washable Multilayer Triboelectric Air Filter for Efficient Particulate Matter PM2.5Removal, Adv. Funct. Mater. 28 (2018) 1706680.

[109] S. Kim, J. Chung, S.H. Lee, J.H. Yoon, D.H. Kweon, W.J. Chung, Tannic acid-functionalized HEPA filter materials for influenza virus capture, Sci. Rep. 11 (2021) 979.

[110] X. Fan, Y. Wang, L. Kong, X. Fu, M. Zheng, T. Liu, W.-H. Zhong, S. Pan, A Nanoprotein-Functionalized Hierarchical Composite Air Filter, ACS Sustain. Chem. Eng. 6 (2018) 11606–11613.

[111] H. Souzandeh, B. Molki, M. Zheng, H. Beyenal, L. Scudiero, Y. Wang, W.H. Zhong, Cross-Linked Protein Nanofilter with Antibacterial Properties for Multifunctional Air Filtration, ACS Appl. Mater. Interfaces 9 (2017) 22846–22855.

[112] C. Wang, J. Fan, R. Xu, L. Zhang, S. Zhong, W. Wang, D. Yu, Quaternary ammonium chitosan/polyvinyl alcohol composites prepared by electrospinning with high antibacterial properties and filtration efficiency, J. Mater. Sci. Technol. 54 (2019) 12522–12532.

[113] M. Pakravan, M.-C. Heuzey, A. Ajji, A fundamental study of chitosan/PEO electrospinning, Polymer 52 (2011) 4813–4824.

[114] B. Zhang, Z.G. Zhang, X. Yan, X.X. Wang, H. Zhao, J. Guo, J.Y. Feng, Y.Z. Long, Chitosan nanostructures by in situ electrospinning for high-efficiency PM2.5 capture, Nanoscale 9 (2017) 4154–4161.

[115] X. Fu, J. Liu, C. Ding, S. Lin, W.H. Zhong, Building bimodal structures by a wettability difference-driven strategy for high-performance protein air-filters, J. Hazard. Mater. 415 (2021), 125742.

[116] L. Zhang, W.-L. Yuan, Z. Zhang, G.-H. Zhang, H. Chen, N. Zhao, L. He, G.-H. Tao, Self-assembled ionic nanofibers derived from amino acids for high-performance particulate matter removal, J. Mater. Chem. A 7 (2019) 4619–4625.

[117] C. Xu, C. Wang, X. He, M. Lyu, S. Wang, L. Wang, Processable graphene oxide-embedded titanate nanofiber membranes with improved filtration performance, J. Hazard. Mater. 325 (2017) 214–222.

[118] K. Zhang, Q. Huo, Y.Y. Zhou, H.H. Wang, G.P. Li, Y.W. Wang, Y.Y. Wang, Textiles/Metal-Organic Frameworks Composites as Flexible Air Filters for Efficient Particulate Matter Removal, ACS Appl. Mater. Interfaces 11 (2019) 17368–17374.

[119] M.-W. Kim, Y.-I. Kim, C. Park, A. Aldalbahi, H.S. Alanazi, S. An, A.L. Yarin, S. S. Yoon, Reusable and durable electrostatic air filter based on hybrid metallized microfibers decorated with metal–organic–framework nanocrystals, J. Mater. Sci. Technol. 85 (2021) 44–55.

[120] W.T. Koo, J.S. Jang, S. Qiao, W. Hwang, G. Jha, R.M. Penner, I.D. Kim, Hierarchical Metal-Organic Framework-Assembled Membrane Filter for Efficient Removal of Particulate Matter, ACS Appl. Mater. Interfaces 10 (2018) 19957–19963.

[121] Y. Dou, W. Zhang, A. Kaiser, Electrospinning of Metal-Organic Frameworks for Energy and Environmental Applications, Adv. Sci. 7 (2020) 1902590.

[122] Z. Su, M. Zhang, Z. Lu, S. Song, Y. Zhao, Y. Hao, Functionalization of cellulose fiber by in situ growth of zeolitic imidazolate framework-8 (ZIF-8) nanocrystals for preparing a cellulose-based air filter with gas adsorption ability, Cellulose 25 (2018) 1997–2008.

[123] J. Guo, A. Hanif, J. Shang, B.J. Deka, N. Zhi, A.K. An, PAA@ZIF-8 incorporated nanofibrous membrane for high-efficiency PM2.5 capture, Chem. Eng. J. 405 (2021), 126584.

[124] J. Li, D. Zhang, T. Yang, S. Yang, X. Yang, H. Zhu, Nanofibrous membrane of graphene oxide-in-polyacrylonitrile composite with low filtration resistance for the effective capture of PM2.5, J. Membr. Sci. 551 (2018) 85–92.

[125] R. Ni, H. Xu, J. Ma, Q. Lu, Y. Hu, C. Huang, Q. Ke, Y. Zhao, Zeolite imidazole framework-8(ZIF-8) decorated keratin-based air filters with formaldehyde removal and photocatalytic disinfection performance, Mater. Today Chem. 23 (2022), 100689.

[126] W. Pan, J.-P. Wang, X.-B. Sun, X.-X. Wang, J.-Y. Jiang, Z.-G. Zhang, P. Li, C.-H. Qu, Y.-Z. Long, G.-F. Yu, Ultra uniform metal–organic framework-5 loading along electrospun chitosan/polyethylene oxide membrane fibers for efficient PM2.5 removal, J. Clean. Prod. 291 (2021) 125270.

[127] T. Li, Z. Zhang, L. Liu, M. Gao, Z. Han, A stable metal-organic framework nanofibrous membrane as photocatalyst for simultaneous removal of methyl orange and formaldehyde from aqueous solution, Colloids Surf. A Physicochem. Eng. Asp. 617 (2021) 126359.

[128] S. Wang, Y. Lin, J. Yang, L. Shi, G. Yang, X. Zhuang, Z. Li, UiO-66-NH2 functionalized cellulose nanofibers embedded in sulfonated polysulfone as proton exchange membrane, Int. J. Hydrog. Energy 46 (2021) 19106–19115.

[129] Z. Wang, C. Zhao, Z. Pan, Porous bead-on-string poly(lactic acid) fibrous membranes for air filtration, J. Colloid Interface Sci. 441 (2015) 121–129.

[130] Y. Yang, S. Zhang, X. Zhao, J. Yu, B. Ding, Sandwich structured polyamide-6/polyacrylonitrile nanonets/bead-on-string composite membrane for effective air filtration, Sep. Purif. Technol. 152 (2015) 14–22.

[131] A. Rajak, D.A. Hapidin, F. Iskandar, M.M. Munir, K. Khairurrijal, Electrospun nanofiber from various source of expanded polystyrene (EPS) waste and their characterization as potential air filter media, Waste Manag. 103 (2020) 76–86.

[132] H. Fong, I. Chun, D.H. Reneker, Beaded nanofibers formed during electrospinning, Polymer 40 (1999) 4585–4592.

[133] M.M. Munir, A.B. Suryamas, F. Iskandar, K. Okuyama, Scaling law on particle-to-fiber formation during electrospinning, Polymer 50 (2009) 4935–4943.

[134] T. Lin, H. Wang, H. Wang, X. Wang, The charge effect of cationic surfactants on the elimination of fibre beads in the electrospinning of polystyrene, Nanotechnology 15 (2004) 1375–1381.

[135] A. Rajak, D.A. Hapidin, F. Iskandar, M.M. Munir, K. Khairurrijal, Controlled morphology of electrospun nanofibers from waste expanded polystyrene for aerosol filtration, Nanotechnology 30 (2019), 425602.

[136] H. Gao, Y. Yang, O. Akampumuza, J. Hou, H. Zhang, X. Qin, A low filtration resistance three-dimensional composite membrane fabricated via free surface electrospinning for effective PM2.5 capture, Environ. Sci. Nano 4 (2017) 864–875.

[137] S.H. Yousefi, H. Vahedi Tafreshi, Modeling electrospun fibrous structures with embedded spacer particles: Application to aerosol filtration, Sep. Purif. Technol. 235 (2020), 116184.

[138] G. Zheng, Z. Shao, J. Chen, J. Jiang, P. Zhu, X. Wang, W. Li, Y. Liu, Self-Supporting Three-Dimensional Electrospun Nanofibrous Membrane for Highly Efficient Air Filtration, Nanomaterials 11 (2021) 2567.

[139] N. Wang, Y. Si, N. Wang, G. Sun, M. El-Newehy, S.S. Al-Deyab, B. Ding, Multilevel structured polyacrylonitrile/silica nanofibrous membranes for high-performance air filtration, Sep. Purif. Technol. 126 (2014) 44–51.

[140] S. Zhang, H. Liu, X. Yin, J. Yu, B. Ding, Anti-deformed Polyacrylonitrile/Polysulfone Composite Membrane with Binary Structures for Effective Air Filtration, ACS Appl. Mater. Interfaces 8 (2016) 8086–8095.

[141] Z. Wang, Z. Pan, Preparation of hierarchical structured nano-sized/porous poly (lactic acid) composite fibrous membranes for air filtration, Appl. Surf. Sci. 356 (2015) 1168–1179.

[142] J. Jiang, Z. Shao, X. Wang, P. Zhu, S. Deng, W. Li, G. Zheng, Three-dimensional composite electrospun nanofibrous membrane by multi-jet electrospinning with sheath gas for high-efficiency antibiosis air filtration, Nanotechnology 32 (2021), 245707.

[143] M. Zhou, M. Fang, Z. Quan, H. Zhang, X. Qin, R. Wang, J. Yu, Large-scale preparation of micro-gradient structured sub-micro fibrous membranes with narrow diameter distributions for high-efficiency air purification, Environ. Sci. Nano 6 (2019) 3560–3578.

[144] J. Choi, B.J. Yang, G.N. Bae, J.H. Jung, Herbal Extract Incorporated Nanofiber Fabricated by an Electrospinning Technique and its Application to Antimicrobial Air Filtration, ACS Appl. Mater. Interfaces 7 (2015) 25313–25320.

[145] N. Wang, Y. Si, J. Yu, H. Fong, B. Ding, Nano-fiber/net structured PVA membrane: Effects of formic acid as solvent and crosslinking agent on solution properties and membrane morphological structures, Mater. Des. 120 (2017) 135–143.

[146] S. Zhang, H. Liu, F. Zuo, X. Yin, J. Yu, B. Ding, A Controlled Design of Ripple-Like Polyamide-6 Nanofiber/Nets Membrane for High-Efficiency Air Filter, Small 13 (2017) 1603151.

[147] H. Liu, S. Zhang, L. Liu, J. Yu, B. Ding, A Fluffy Dual-Network Structured Nanofiber/Net Filter Enables High-Efficiency Air Filtration, Adv. Funct. Mater. 29 (2019) 1904108.

[148] H. Liu, S. Zhang, L. Liu, J. Yu, B. Ding, High-performance filters from biomimetic wet-adhesive nanoarchitectured networks, J. Mater. Chem. A 8 (2020) 18955–18962.

[149] H. Liu, S. Zhang, L. Liu, J. Yu, B. Ding, High-Performance PM 0.3 Air Filters Using Self-Polarized Electret Nanofiber/Nets, Adv. Funct. Mater. 30 (2020) 1909554.

[150] N. Tang, Y. Chen, Y. Li, B. Yu, 2D Polymer Nanonets: Controllable Constructions and Functional Applications, Macromol. Rapid Commun. (2022) e2200250.

[151] Z. Li, Y. Xu, L. Fan, W. Kang, B. Cheng, Fabrication of polyvinylidene fluoride tree-like nanofiber via one-step electrospinning, Mater. Des. 92 (2016) 95–101.

[152] Z. Li, W. Kang, H. Zhao, M. Hu, J. Ju, N. Deng, B. Cheng, Fabrication of a polyvinylidene fluoride tree-like nanofiber web for ultra high performance air filtration, RSC Adv. 6 (2016) 91243–91249.

[153] Z. Shao, Y. Chen, J. Jiang, Y. Xiao, G. Kang, X. Wang, W. Li, G. Zheng, Multistage-Split Ultrafine Fluffy Nanofibrous Membrane for High-Efficiency Antibacterial Air Filtration, ACS Appl. Mater. Interfaces 14 (2022) 18989–19001.

[154] J. Song, B. Zhang, Z. Lu, Z. Xin, T. Liu, W. Wei, Q. Zia, K. Pan, R.H. Gong, L. Bian, Y. Li, J. Li, Hierarchical Porous Poly(l-lactic acid) Nanofibrous Membrane for Ultrafine Particulate Aerosol Filtration, ACS Appl. Mater. Interfaces 11 (2019) 46261–46268.

[155] F. Xie, Y. Wang, L. Zhuo, F. Jia, D. Ning, Z. Lu, Electrospun Wrinkled Porous Polyimide Nanofiber-Based Filter via Thermally Induced Phase Separation for Efficient High-Temperature PMs Capture, ACS Appl. Mater. Interfaces 12 (2020) 56499–56508.

[156] E. des Ligneris, L. F. Dumee, R. Al-Attabi, E. Castanet, J. Schutz, L. Kong, Mixed Matrix Poly(Vinyl Alcohol)-Copper Nanofibrous Anti-Microbial Air-Microfilters, Membranes 9 (2019) 87.

[157] Y. Deng, T. Lu, J. Cui, W. Ma, Q. Qu, X. Zhang, Y. Zhang, M. Zhu, R. Xiong, C. Huang, Morphology engineering processed nanofibrous membranes with secondary structure for high-performance air filtration, Sep. Purif. Technol. 294 (2022), 121093.

[158] F. Xie, Y. Wang, L. Zhuo, D. Ning, N. Yan, J. Li, S. Chen, Z. Lu, Multiple hydrogen bonding self-assembly tailored electrospun polyimide hybrid filter for efficient air pollution control, J. Hazard. Mater. 412 (2021), 125260.

[159] D. Lv, R. Wang, G. Tang, Z. Mou, J. Lei, J. Han, S. De Smedt, R. Xiong, C. Huang, Ecofriendly Electrospun Membranes Loaded with Visible-Light-Responding Nanoparticles for Multifunctional Usages: Highly Efficient Air Filtration, Dye Scavenging, and Bactericidal Activity, ACS Appl. Mater. Interfaces 11 (2019) 12880–12889.

[160] G. Zheng, H. Peng, J. Jiang, G. Kang, J. Liu, J. Zheng, Y. Liu, Surface Functionalization of PEO Nanofibers Using a TiO2 Suspension as Sheath Fluid in a Modified Coaxial Electrospinning Process, Chem. Res. Chin. Univ. 37 (2021) 571–577.

[161] M. Li, Y. Feng, K. Wang, W.F. Yong, L. Yu, T.S. Chung, Novel Hollow Fiber Air Filters for the Removal of Ultrafine Particles in PM2.5 with Repetitive Usage Capability, Environ. Sci. Technol. 51 (2017) 10041–10049.

[162] J. Liu, X. Zhang, H. Zhang, L. Zheng, C. Huang, H. Wu, R. Wang, X. Jin, Low resistance bicomponent spunbond materials for fresh air filtration with ultra-high dust holding capacity, RSC Adv. 7 (2017) 43879–43887.

[163] Q. Su, Z. Wei, C. Zhu, X. Wang, W. Zeng, S. Wang, S. Long, J. Yang, Multilevel structured PASS nanofiber filter with outstanding thermal stability and excellent mechanical property for high-efficiency particulate matter removal, J. Hazard. Mater. 431 (2022), 128514.

[164] W. Xu, Y. Chen, Y. Liu, Directional Water Transfer Janus Nanofibrous Porous Membranes for Particulate Matter Filtration and Volatile Organic Compound Adsorption, ACS Appl. Mater. Interfaces 13 (2021) 3109–3118.

[165] Z. Shao, J. Chen, L.J. Ke, Q. Wang, X. Wang, W. Li, G. Zheng, Directional Transportation in a Self-Pumping Dressing Based on a Melt Electrospinning Hydrophobic Mesh, ACS Biomater. Sci. Eng. 7 (2021) 5918–5926.

[166] Z. Shao, Q. Wang, J. Chen, J. Jiang, X. Wang, W. Li, G. Zheng, Directional Water Transport Janus Composite Nanofiber Membranes for Comfortable Bioprotection, Langmuir 38 (2022) 309–319.

[167] L. Hou, J. Liu, D. Li, Y. Gao, Y. Wang, R. Hu, W. Ren, S. Xie, Z. Cui, N. Wang, Electrospinning Janus Nanofibrous Membrane for Unidirectional Liquid Penetration and Its Applications, Chem. Res. Chin. Univ. 37 (2021) 337–354.

[168] X. Tian, H. Jin, J. Sainio, R.H.A. Ras, O. Ikkala, Droplet and Fluid Gating by Biomimetic Janus Membranes, Adv. Funct. Mater. 24 (2014) 6023–6028.

[169] L. Shi, X. Liu, W. Wang, L. Jiang, S. Wang, A Self-Pumping Dressing for Draining Excessive Biofluid around Wounds, Adv. Mater. 31 (2019) e1804187.

[170] X. Zhao, Y. Li, T. Hua, P. Jiang, X. Yin, J. Yu, B. Ding, Cleanable Air Filter Transferring Moisture and Effectively Capturing PM2.5, Small 13 (2017) 1603306.

[171] Z. Wang, Y. Zhang, X.Y.D. Ma, J. Ang, Z. Zeng, B.F. Ng, M.P. Wan, S.-C. Wong, X. Lu, Polymer/MOF-derived multilayer fibrous membranes for moisture-wicking and efficient capturing both fine and ultrafine airborne particles, Sep. Purif. Technol. 235 (2020) 116183.

[172] Y. Yang, R. He, Y. Cheng, N. Wang, Multilayer-structured fibrous membrane with directional moisture transportability and thermal radiation for high-performance air filtration, e-Polymers 20 (2020) 282–291.

[173] Q. Li, Y. Yin, D. Cao, Y. Wang, P. Luan, X. Sun, W. Liang, H. Zhu, Photocatalytic Rejuvenation Enabled Self-Sanitizing, Reusable, and Biodegradable Masks against COVID-19, ACS Nano (2021) 11992–12005.

[174] M. Zhu, D. Hua, H. Pan, F. Wang, B. Manshian, S.J. Soenen, R. Xiong, C. Huang, Green electrospun and crosslinked poly(vinyl alcohol)/poly(acrylic acid) composite membranes for antibacterial effective air filtration, J. Colloid Interface Sci. 511 (2018) 411–423.

[175] W.A. Abbas, B.S. Shaheen, L.G. Ghanem, I.M. Badawy, M.M. Abodouh, S. M. Abdou, S. Zada, N.K. Allam, Cost-Effective Face Mask Filter Based on Hybrid Composite Nanofibrous Layers with High Filtration Efficiency, Langmuir 37 (2021) 7492–7502.

[176] L. Zhang, L. Li, L. Wang, J. Nie, G. Ma, Multilayer electrospun nanofibrous membranes with antibacterial property for air filtration, Appl. Surf. Sci. 515 (2020), 145962.

[177] N.A. Patil, P.M. Gore, N. Jaya Prakash, P. Govindaraj, R. Yadav, V. Verma, D. Shanmugarajan, S. Patil, A. Kore, B. Kandasubramanian, Needleless electrospun phytochemicals encapsulated nanofibre based 3-ply biodegradable mask for combating COVID-19 pandemic, Chem. Eng. J. 416 (2021) 129152.

[178] A. Giordano, G. Tommonaro, Curcumin and Cancer, Nutrients 11 (2019) 2376.

[179] M. Abbas, T. Hussain, M. Arshad, A.R. Ansari, A. Irshad, J. Nisar, F. Hussain, N. Masood, A. Nazir, M. Iqbal, Wound healing potential of curcumin cross-linked chitosan/polyvinyl alcohol, Int. J. Biol. Macromol. 140 (2019) 871–876.

[180] Y. Xiao, Y. Wang, W. Zhu, J. Yao, C. Sun, J. Militky, M. Venkataraman, G. Zhu, Development of tree-like nanofibrous air filter with durable antibacterial property, Sep. Purif. Technol. 259 (2021) 118135.

[181] Y. Zhang, S. Yuan, X. Feng, H. Li, J. Zhou, B. Wang, Preparation of Nanofibrous Metal-Organic Framework Filters for Efficient Air Pollution Control, J. Am. Chem. Soc. 138 (2016) 5785–5788.

[182] V. Kadam, Y.B. Truong, J. Schutz, I.L. Kyratzis, R. Padhye, L. Wang, Gelatin/beta-Cyclodextrin Bio-Nanofibers as respiratory filter media for filtration of aerosols and volatile organic compounds at low air resistance, J. Hazard. Mater. 403 (2021), 123841.

[183] M. Hu, L. Yin, N. Low, D. Ji, Y. Liu, J. Yao, Z. Zhong, W. Xing, Zeolitic-imidazolate-framework filled hierarchical porous nanofiber membrane for air cleaning, J. Membr. Sci. 594 (2020), 117467.

[184] V. Kadam, Y.B. Truong, C. Easton, S. Mukherjee, L. Wang, R. Padhye, I.L. Kyratzis, Electrospun Polyacrylonitrile/β-Cyclodextrin Composite Membranes for Simultaneous Air Filtration and Adsorption of Volatile Organic Compounds, ACS Appl. Nano Mater. 1 (2018) 4268–4277.

[185] B. Liu, S. Zhang, X. Wang, J. Yu, B. Ding, Efficient and reusable polyamide-56 nanofiber/nets membrane with bimodal structures for air filtration, J. Colloid Interface Sci. 457 (2015) 203–211.

[186] J. Xiong, A. Li, Y. Liu, L. Wang, X. Qin, J. Yu, Multi-Scale Nanoarchitectured Fibrous Networks for High-Performance, Self-Sterilization, and Recyclable Face Masks, Small 18 (2022) e2105570.

[187] Y. Liu, S. Li, W. Lan, M.A. Hossen, W. Qin, K. Lee, Electrospun antibacterial and antiviral poly(ε-caprolactone)/zein/Ag bead-on-string membranes and its application in air filtration, Mater. Today Adv. 12 (2021), 100173.

[188] C. Pei, Q. Ou, D.Y.H. Pui, Effects of temperature and relative humidity on laboratory air filter loading test by hygroscopic salts, Sep. Purif. Technol. 255 (2021), 117679.

[189] Z. Cui, L. Kang, L. Li, L. Wang, K. Wang, A combined state-of-charge estimation method for lithium-ion battery using an improved BGRU network and UKF, Energy 259 (2022), 124933.

[190] C. Liu, D. Li, L. Wang, L. Li, K. Wang, Strong robustness and high accuracy in predicting remaining useful life of supercapacitors, APL Mater. 10 (2022), 061106.

[191] Z. Cui, L. Kang, L. Li, L. Wang, K. Wang, A hybrid neural network model with improved input for state of charge estimation of lithium-ion battery at low temperatures, Renewable Energy 198 (2022) 1328–1340.

[192] Z. Yi, K. Zhao, J. Sun, L. Wang, K. Wang, Y. Ma, A. Ahmadian, Prediction of the Remaining Useful Life of Supercapacitors, Math. Problems Eng. 2022 (2022) 1–8.